A Satellite-linked Tag for the Long-term Monitoring of Diving Behavior in Large Whales

Daniel M. Palacios (daniel.palacios@oregonstate.edu)
Oregon State University https://orcid.org/0000-0001-7069-7913
Ladd M. Irvine
Oregon State University
Barbara A. Lagerquist
Oregon State University
James A. Fahlbusch
Stanford University Hopkins Marine Station
John Calambokidis
Cascadia Research Collective
Stanley M. Tomkiewicz
Telonics, Inc
Bruce R. Mate
Oregon State University

Research Article

Keywords: Argos satellite telemetry, bio-logging, smart tags, accelerometry, adaptive algorithm, event detection, diving behavior, lunge-feeding, rorqual whales, cetaceans

Posted Date: August 31st, 2021

DOI: https://doi.org/10.21203/rs.3.rs-834159/v1

A satellite-linked tag for the long-term monitoring of diving behavior in large whales

Daniel M. Palacios[1,2,†,*], Ladd M. Irvine[1,2,†], Barbara A. Lagerquist[1,2], James A. Fahlbusch[3,4], John Calambokidis[4], Stanley M. Tomkiewicz[5] and Bruce R. Mate[1,2]

[1]Marine Mammal Institute, Oregon State University, Newport, Oregon, USA

[2]Department of Fisheries, Wildlife, and Conservation Sciences, Oregon State University, Newport, Oregon, USA

[3]Department of Biology, Hopkins Marine Station, Stanford University, Pacific Grove, California, USA

[4]Cascadia Research Collective, Olympia, Washington, USA

[5]Telonics, Inc., Mesa, Arizona, 85204, USA

[†]These two authors contributed equally

*Corresponding author:

Daniel M. Palacios

daniel.palacios@oregonstate.edu

Abstract

Despite spending much of their time on activities underwater, the technology in use to track whales over large geographic ranges via satellite has been largely limited to locational data, with most applications focusing on characterizing their horizontal movements. We describe the development of the RDW tag, a new Argos-based satellite telemetry device that incorporates sensors for monitoring the movements and dive behavior of large whales over several months without requiring recovery. Based on an implantable design, the tag features a saltwater conductivity switch, a tri-axial accelerometer, and an optional pressure transducer, along with onboard software for data processing and detection of behavioral events or activities of interest for transmission. We configured the software to detect dives and create per-dive summaries describing behavioral events associated with feeding activities in rorqual whales. We conducted a validation by proxy of the dive summary and event detection algorithms using data from a medium-duration archival tag. The dive summary algorithm accurately reported dive depth and duration, while the accuracy of the lunge-feeding event detection algorithm was dependent on the precision of the accelerometer data that was used, with a predicted accuracy of 0.74 for correctly classifying feeding dives from 1/64-G precision data and 0.95 from 1-mG precision data. We also present data from field deployments of the tag on seven humpback whales (*Megaptera novaeangliae*) and one blue whale (*Balaenoptera musculus*). The eight tags transmitted over a median tracking period of 17.5 d (range: 3.9-76.4 d) across both species. The median proportion of the tracking period summarized by received dives for the eight tags was 50.4% (range: 11.1-88.7%). The median number of received dives per day was 76.5 (range: 1-191). The results documented diel and longer-term variability in diving and feeding behavior, showing marked differences within and among individuals tracked contemporaneously. By

monitoring the per-dive behavior of large whales over multi-month timescales of movement, the RDW tags provided some of the first assessments of previously unobservable behaviors across entire geographic ranges, linking local-scale behavior to broader, ecosystem-scale processes. The RDW tag extends the applications of whale satellite telemetry to new areas of physiology, ecology, and conservation.

Keywords

Argos satellite telemetry, bio-logging, smart tags, accelerometry, adaptive algorithm, event detection, diving behavior, lunge-feeding, rorqual whales, cetaceans

Background

The field of wildlife tracking and bio-logging using electronic devices has experienced explosive growth in the last two decades thanks to important technological advances and decreasing costs, which have made it a widely accessible approach for the study of movement, both in terrestrial and aquatic animals (1,2). Despite the dawn of this "golden age of animal tracking," large whales remain among the most difficult species to study using these technologies. This is due to the fact that deploying and recovering electronic devices at sea on large, highly streamlined animals that cannot be captured for tag attachment and that have the capability to move great distances in short periods of time involves complicated and expensive logistics (3). Furthermore, like with other air-breathing aquatic animals that spend most of their time underwater, data transmission to earth-orbiting satellite platforms is limited to the brief instants that a whale is at the surface. This situation has led to a dearth of behavioral data at several spatio-temporal scales, which has

limited the scope of questions that can be currently addressed on whale distribution, movement, and ecology.

The primary technology for tracking the long-distance movements of large whales, in use since 1997, has been a "consolidated" tag design (*sensu* (4)) linked to the Argos satellite system, where the electronics and retention elements are incorporated into a single implantable tag body from which only the antenna and a saltwater switch (SWS; which ensures transmissions only occur when the animals are at the surface) are external to minimize hydrodynamic drag (3,5,6). These non-recoverable tags can stay attached for long periods of time (typically several months) before they fall off, although narrow bandwidth limits the amount of data they can transmit through the Argos system, so their primary use has been for geographic localization. Some consolidated tag models have included capabilities for reporting surfacing intervals and summarized dive behavior data in the form of time spent in discrete depth or temperature intervals (i.e., "histogram data") or as per-dive metrics such as dive duration and maximum dive depth (7–11). However, to date, a direct measure of feeding behavior activity has not been available in consolidated, long-duration whale tags.

Most of what we know about large whale diving behavior comes from short- and medium-duration archival tags, which permit collection of continuous, sensor-rich data streams. For example, from these bio-loggers we have learned that prey capture events in several whale species are associated with rapid changes in motion that can be identified by their stereotypical signatures in accelerometer data (12–15). This information has been used to examine topics like the kinematics of feeding behavior (16–18), feeding strategies in relation to the local prey field (19–23), or behavioral responses in the context of interactions with anthropogenic activities (24–27). However, the typical deployment period of these devices is limited to < 24 h (if attached

87 with suction cups) or to a few days or weeks (if attached with subdermal anchors), and recovery
88 of the tags is required for download of the complete data record (24,27–31).

89 Whale foraging behavior at broader scales has only been inferred indirectly from tracking data,
90 either from the characteristics of horizontal movement (32) or from diving depth (7,8). However,
91 the relationship between inferred and direct measurements of whale feeding behavior activity
92 across spatial and temporal scales remains unverified (33). As movement behavior is driven by
93 resource tracking and food acquisition through a hierarchy of processes that operate at multiple
94 spatio-temporal scales (34), obtaining this information is essential to quantify the variability of
95 resource dynamics and foraging strategies, to test predictions on emergent movement behavior,
96 and to improve our overall understanding of the structure and function of global aquatic
97 ecosystems (2,35). More than ever, this information can be critical to guide biodiversity
98 conservation in the face of rapid global change (1,2,35).

99 Here we present a new satellite telemetry device for tracking the movements and dive behavior
100 of large whales over several months without requiring recovery. The tag, manufactured by
101 Telonics, Inc. (Mesa, Arizona, USA), collects dive duration from a SWS, inertial motion from a
102 tri-axial accelerometer, and dive depth from a pressure transducer. The tag uses a
103 microprocessor-based approach (36) featuring data processing software for (a) detecting
104 behavioral events from accelerometer data using an adaptive algorithm to account for individual
105 variation in behavior, and (b) summarizing and compressing dive data streams for transmission
106 through the Argos system. While satellite-linked tag platforms featuring accelerometers and
107 associated software have been recently developed for detecting, abstracting, and transmitting
108 behavioral measures of activity in other marine top predators (37–39), this is the first time that

accelerometers with event detection software are used on a satellite-transmitting tag for large whales.

Methods

Tag development

Development of the tag proceeded incrementally between 2015 and 2017, during which time we tested a variety of tag and software configurations in collaboration with Telonics. The initial model (RDW-640) used the SWS sensor to monitor and report dive duration through Argos. This model also included a tri-axial accelerometer, but the software for processing this data stream was not yet developed, so the sensor was not active. A subsequent model (RDW-665) added a pressure sensor, increased battery capacity, and implemented a behavioral event detection algorithm to analyze the accelerometer data stream in real time. The updated model generated a data summary for every dive, consisting of dive duration, maximum dive depth, and number of behavioral events detected. Software onboard the tag's microprocessor packaged these summaries into messages for transmission through Argos, completing the development of the device. As the RDW-665 model included all components and configurations that were used by the RDW-640 model, from this point forward we refer to all tag versions as the "RDW tag" unless specifically noted.

Tag components and design

The tag followed the same design of other consolidated tags for large whales in use since 1997 (3), which consists of a main body, an antenna and external sensor endcap at the distal end, a penetrating tip at the proximal end, and an anchoring system (Figure 1). The main body

consisted of a stainless-steel cylinder 18.8 cm in length × 1.9 cm in diameter that housed a motherboard, a certified Argos transmitter (401.650 MHz ± 30 kHz operational frequency), a thermistor for internal tag temperature monitoring, a tri-axial accelerometer, and a lithium battery pack (two DL2/3A Duracell® 1550 mAh 3 V cells in parallel). An external flexible whip antenna (15.8-cm long) and a stalked SWS (2.2-cm long), both constructed of single-strand nitinol (1.27 mm in diameter), were connected to the transmitter and mounted on a polycarbonate endcap (2.5 cm in external length) that sealed the distal end of the cylinder with two O-rings. The port for the pressure sensor of the RDW-665 model was also mounted on the endcap (Figure 1).

The endcap had two perpendicular stops (1.5 cm long × 0.9 cm wide × 0.6 cm thick) extending laterally to prevent tags from embedding too deeply on deployment or from migrating inward after deployment. The penetrating tip was attached to the main body by a threaded screw (1.17 cm long × 0.64 cm in diameter) and fixed with a setscrew to prevent unthreading after deployment. It consisted of a polyoxymethylene (Delrin®) nose cone into which a ferrule shaft with four double-edged blades was pressed and secured with a transverse roll-pin to prevent unintentional removal. The anchoring system consisted of two rows of outwardly curved metal strips (each strip was 3.2 cm long × 0.6 cm wide) mounted on the main body at the nose cone (proximal) end (Figure 1). Total tag weight was approximately 300 g.

The tag's cylinder was partially coated with a long-dispersant polymer matrix (Resomer® or Eudragit®) in which a broad-spectrum antibiotic (gentamicin sulfate) was mixed to allow for a continual release of antibiotic into the tag site for an extended time to reduce the chances of infection (Figure 1). Like other consolidated tags, the RDW tag was designed to be almost completely implantable (except for the perpendicular stops, antenna, and SWS), and was

153 ultimately shed from the whale due to hydrodynamic drag and/or the natural migration out of the
154 tissue as a foreign body response (3).

155 *Tag sensors*

156 The tag used a SWS to synchronize Argos transmissions with surfacings and suppress them
157 while animals were underwater to save battery power (36). The status of the SWS (wet/dry) was
158 used to record dive start and end times and calculate dive duration. An onboard pressure
159 transducer allowed collection of dive depth data with an accuracy of ±2 m or ±1% of recorded
160 depth, whichever was greater. A tri-axial accelerometer was also included, and recorded data at
161 8-bit precision (1/64 G), with an accuracy of ±0.003 G. The sampling rate of tag sensors was
162 user-programmable and for our trials it was set to 1 Hz (1 s) for the SWS, 0.2 Hz (5 s) for the
163 pressure transducer, and 4 Hz (0.25 s) for the accelerometer.

164 *Tag software*

165 *(a) Dive summary algorithm:*

166 Dive behavior was recorded and summarized for "selected dives," defined as dives meeting user-
167 specified criteria for depth and duration, to generate "dive summaries". For the tag deployments
168 presented here, selected dives were identified as dives > 2 min in duration and > 10 m in depth.
169 Summary parameters including the start date, time, and duration of each selected dive were
170 recorded, along with the maximum depth of the dive. Other possible dive depth-related metrics
171 could be reported by the tag, like the profile of individual dives or the percentage of time spent in
172 user-defined depth bins, but we did not record them in this study. The tag could optionally be
173 programmed for behavior event detection within selected dives (see next section), using the

174 accelerometer to detect marked changes in motion, such as lunge-feeding events, or as a more
175 general measure of activity based on variability of the accelerometer data, with the results
176 included in the dive summary.

177 *(b) Event detection algorithm:*

178 Accelerometer sensor data were processed by the tag's microprocessor using an adaptive event
179 detection algorithm. Threshold parameters for the event detection algorithm were continually
180 updated from the sensor data stream and informed future iterations of the algorithm, allowing it
181 to adapt over time. This adaptability can account, among other things, for differences in tag
182 placement on the whale's body, which can affect the magnitude of a sensor's signal owing to
183 site-specific differences in acceleration and mechanical processes (14,40,41). The event
184 detection algorithm was specifically developed to detect lunge-feeding behavior in rorqual
185 whales (family Balaenopteridae), which produces strong stereotypical signatures in acceleration
186 data (42,43) that can be used as a measure of feeding effort.

187 Lunge-feeding events were derived from the change in the acceleration vector ("jerk"), which is
188 typically calculated as the norm of the difference in consecutive acceleration readings during
189 selected dives (16). However, for this application the jerk calculation was integrated over a full
190 second by subtracting the current accelerometer readings from those one second previous. This
191 variation was used to standardize the units to 1 s and to reduce the effect of spurious readings.
192 Additionally, accelerometer readings from the first 5 s and final 5 s of each selected dive were
193 excluded to eliminate artifacts from fluke stroking associated with the start or end of a dive (16),
194 as well as from ocean surface wave drag (18).

195 The development of the event detection algorithm went through two iterations:

196 Version 1: A study by Simon et al. (16) showed that rorqual feeding lunges produce distinct
197 peaks in jerk, so the initial event detection algorithm identified jerk values that exceeded the
198 mean jerk by a threshold of 3.5 standard deviations (sd), with a 30 s blanking time (14) between
199 identified events to account for prey handling. Software in the tag's microprocessor allowed
200 mean and sd of jerk values to be continually updated following each selected dive, making them
201 the running mean and sd of jerk up to that point. By updating criteria to identify lunge-feeding
202 events, the algorithm was able to adapt over time and converge on threshold values that better
203 accounted for individual differences in accelerometer readings.

204 Version 2: A subsequent study by Allen et al. (13) indicated that rorqual feeding lunges were
205 best characterized by a maximum followed by a minimum in jerk, so in 2017 the event detection
206 algorithm was updated to identify instances when the jerk value exceeded a threshold of 1.5 sd
207 above the mean, followed by a value less than one half of the mean occurring within 30 s after
208 the jerk peak. Jerk values had to exceed the upper threshold for 2 s to qualify as a lunge-feeding
209 event, to account for error or values close to the cut-off. Lunge-feeding events for each selected
210 dive were then counted after applying a 35 s blanking time. As with version 1, the threshold
211 mean and sd jerk values were updated following each selected dive.

212 *(c) Data transmission via Argos:*

213 The RDW tag made use of a highly compressed data transmission protocol to increase
214 throughput of summarized dive data via Argos. Dive summaries were collected into "dive
215 summary messages," consisting of a variable number of consecutive (typically 4-10) selected
216 dives, depending on the number of reported summary parameters and other data compression
217 factors like the differences in the values of data being reported. The tag maintained a buffer that

held up to ten dive summary messages in the tag's microprocessor random-access memory. When enough dive summaries were recorded to create a new dive summary message, it was added to the buffer. If there were already ten messages in the buffer, the oldest message was discarded to make space for the new message.

Tag transmissions could contain either one dive summary message (randomly selected from the buffer) or a utility message containing the tag's current internal temperature and voltage for diagnostic purposes. The update to version 2 of the event detection algorithm also added the current jerk mean and sd values into utility messages to monitor trends in those criteria over time. For this study, tags were programmed to transmit for six one-hour periods each day, with a 10-s repetition rate, and scheduled to coincide with the most likely times an Argos satellite would be overhead, giving a conservative expected functional life of 104-161 d.

Validation approach

Sensor functionality

During development, we tested prototype tags in the laboratory to evaluate sensor functionality and ability to accurately report dive summaries through the Argos system. We evaluated the tag's ability to record diving behavior by simulating dives of varying durations and depths by closing the SWS and placing the tags in a pressurized chamber to replicate water depth. Enough dives were simulated to fill multiple dive summary messages, which were then transmitted during an Argos satellite pass. Recovered dive summaries showed good agreement with corresponding simulated dives. Additionally, diagnostic software in the tag allowed direct download of a short-duration segment of the continuous accelerometer record, which we used to

confirm the sensor's ability to record rapid changes in orientation and acceleration resulting from a person manipulating the tag to simulate abrupt motion changes.

Dive summary and event detection algorithms

In principle, field validation of data collected by the RDW tag would involve a quantitative comparison of the dive summaries obtained through Argos with equivalent summaries generated from the data recorded onboard the tag after a deployment. However, consolidated tags are not designed for recovery, so this was not an option. Alternatively, a comparison could be made with a data record from a second archival device deployed on the same animal and later recovered for analysis. However, this option was not viable during tag development due to financial constraints and logistical challenges associated with placing multiple tags on a single whale.

Instead, we implemented a proxy validation of the tag's dive summary and event detection algorithms. For this purpose, we used a continuous data record from a Wildlife Computers TDR10-F medium-duration archival tag (hereafter "TDR10 archival data") deployed on a blue whale (*Balaenoptera musculus*) for 17.8 d while it was foraging off southern California in summer 2017 (24,30). We examined the performance of the RDW tag dive summary and event detection algorithms by running the TDR10 archival data record through the RDW tag's algorithms and comparing this output to the corresponding "true" dive summaries calculated from the TDR10 archival data using standard analytical workflows for dive data. Analyses were implemented in the R software for statistical computing, v. 4.0.2 (44).

As the TDR10 archival tag continuously recorded pressure (depth) and tri-axial accelerometer data at 32 Hz, we decimated the sensor data to 4 Hz to match the sampling rate of the RDW tag. Additionally, the TDR10 archival accelerometer data were recorded with a native precision of 1

mG, so we subsequently reduced it to 1/64 G to match the precision of the RDW tag observations. We identified "TDR10 dives" as those > 10 m depth using the *find_dives()* function from the R package *tagtools* (https://github.com/stacyderuiter/TagTools; (14)). We then calculated the maximum dive depth and dive duration for each dive, as well as their start and end times using custom R scripts. Feeding lunges were identified manually using stereotypical kinematic signatures from the 32-Hz accelerometer data (i.e., the animal's depth, pitch, roll, and speed, *sensu* (45)).

We used the RDW dive summary and event detection algorithms to generate dive summaries from the TDR10 archival data (hereafter "RDW dives") as they would be received through Argos during an *in-situ* deployment (i.e., dive start date-time, maximum dive depth, dive duration, and number of lunge-feeding events). To validate the RDW dive summary algorithm, we matched true dive summaries from the TDR10 dives to corresponding RDW dives using the dive start date-times and tested the correspondence of reported maximum dive depth and dive duration values with linear regression. For the number of lunge-feeding events per dive, we used polychoric correlation to assess the relationship between the number of RDW-detected lunge-feeding events and the number of "known" feeding lunges identified in the TDR10 archival data summary. This analysis provided an approximation of a Pearson's correlation coefficient for two ordinal variables and was conducted using the R package *polycor* v. 0.7-10 (46). We also calculated the "miss rate" per dive as the number of false negatives in the RDW-detected lunge feeding events divided by the number of known feeding lunges from the TDR10 archival data summary.

The RDW tag was developed to monitor large whale feeding behavior across ecologically relevant spatio-temporal scales (i.e., 10s to 1000s of km and days to months). These scales are

hierarchical in nature (34), such that the per-dive aspects of feeding behavior (e.g., the number of lunge-feeding events) should scale up to daily feeding intensity (e.g., bouts of feeding dives), which, in turn, should give rise to regional patterns of elevated feeding effort as a function of resource availability (34,47). We evaluated the ability of RDW data to accurately portray feeding behavior at multiple scales of interest by (a) identifying feeding dives (i.e., dives with at least one lunge-feeding event), and (b) empirically characterizing bouts of multiple feeding dives. To assess the ability of RDW-derived lunge-feeding events to correctly identify feeding dives in relation to "known" feeding dives identified from the TDR10 archival data, we derived a confusion matrix and calculated the classification's accuracy rate along with its binomial proportion 95% confidence interval (CI) using function *confusionMatrix()* in R package *caret* v. 6.0-86 (48). To validate how the RDW data scaled up to feeding intensity, we assessed the temporal trends in the number of feeding dives obtained from the RDW and TDR10 dive summaries through log-survivorship analysis (22,49,50). This analysis consisted of graphically representing the number of feeding dive sequences ("bouts") for each summary as a function of the time between feeding dives, with the goal of identifying a point where the number of bouts stabilized as the time between feeding dives increased, indicating the characteristic scale of foraging as a criterion to differentiate between bouts (22). We validated the RDW-derived log survivorship plot by visually comparing it for consistency with one generated from TDR10 data. Probability density plots of the time between feeding dives are also useful to identify a bout criterion, so we also tested the RDW-derived probability density distribution of time between feeding dives for consistency with the distribution of values from TDR10 data using the Bhattacharyya's similarity coefficient (51,52), where values < 0.05 and > 0.95 indicate that the distributions are significantly different, or similar, respectively, and intermediate values can

indicate the probability of overlap between the distributions (51). Bouts were identified based on a common criterion of time between feeding dives identified from the log-survivorship analysis. The number of RDW-derived bouts was then compared to the number of true TDR10-derived bouts to assess how well RDW dive summaries could represent broader-scale metrics of feeding. As indicated above, the precision of the accelerometer sensor of the RDW tags used in field deployments was limited to 1/64 G, while the TDR10 accelerometer data were natively recorded at 1 mG. This allowed us to repeat the proxy validation process described above at the higher precision to determine if sensor precision influenced the accuracy of the RDW event detection algorithm, offering the opportunity to improve future versions of the tag.

Field deployments

Tagging operations were conducted on humpback whales (*Megaptera novaeangliae)* in southeastern Alaska from 8-17 November 2015, on blue whales in southern California from 6-20 July 2016, and on humpback whales in central California from 21 July - 5 August 2017. Tags were deployed from a 6.7-m rigid-hulled inflatable boat. Candidate whales for tagging were selected based on visual observation of body condition. No whales were tagged that appeared emaciated or that were extensively covered by external parasites. Tags were implanted on the whales from distances of 2 to 4 m using the Air Rocket Transmitter System, a pneumatic applicator with adjustable pressure (typically 90-100 psi [6.2-6.9 bar]), modified for projectile tags (3,5). Tags were placed on the whales' back close to the mid-line, where they would clear the water for satellite transmission as the whales surfaced to breathe.

When possible, skin and blubber biopsy samples were collected simultaneous to tagging (on the same surfacing) using a stainless-steel tipped dart delivered by a crossbow (53) for genetic sex

identification based on amplification of regions of the X and Y chromosomes (54,55). Photographs of the tagged whales were also collected whenever possible for individual identification (56,57). Full details of these field operations are reported in Palacios et al. (58) and Mate et al. (59,60).

Proportion of the tracking period summarized by received dives

The proportion of the tracking period summarized by received dives from all deployed RDW tags was calculated as the sum of all received dive durations, *d*, plus the sum of all post-dive intervals at the surface, *s* (i.e., the time between the end of one selected dive and the start of the next one), divided by the total tracking duration for each tag record. We only calculated *s* for dives reported within the same transmission because we could not be sure dives were sequential from one transmission to the next (e.g., if there was a 15-min time difference between the end of the last dive in one received transmission and the start of the first dive of the next received transmission, it is possible the whale made no selected dives during that time, or made a series of short-duration selected dives that were packaged into a transmission that was not received).

Assessment of temporal variation in dive behavior

To characterize variability of whale dive behavior over time, we calculated two metrics for dive performance: 1) The proportion of time spent underwater, *U*, as:

$$U = d/(d + s),$$

and 2) the ratio of the cumulative sums of *s* and *d* over the tracked period, r_i, as:

$$\boldsymbol{r_i = \sum_{k=1}^{i} s_k / \sum_{k=1}^{i} d_k},$$

for $i = 1, 2, \ldots, N$ dives received over the tracked period.

The cumulative r_i ratio contrasts surface recovery time to diving time and thus represents a running index of diving capacity over time.

Location assignment for received dives

A location filtering protocol was implemented on the received Argos locations prior to constructing a track to mitigate for locations with large estimation error and to improve confidence in where identified dive behaviors were observed (61). The raw Argos locations were filtered to remove the lowest-quality location classes (Z and B from one message). Locations from redundant satellite passes were also removed and a 14-km/h swim speed filter was applied to remove locations that would require the whale to travel at an unreasonably high speed. A location was then assigned to each reported dive by the RDW tags based on the start time of the dive and the temporally closest filtered Argos location. Locations of dives more than 10 min from an Argos location were estimated by linear interpolation between the temporally closest Argos locations before and after the dive occurred using the dive time to determine where on the line the dive should fall (61).

Results

Proxy validation of dive summary data

1/64-G precision data

The RDW dive summary algorithm identified 2,462 selected dives and 1,302 lunge-feeding events (range = 0-11 per dive; Figure A1 in Additional file) when implemented on TDR10

369 archival data at the reduced precision of the accelerometer sensor of the RDW tags used in field
370 deployments (1/64 G). A total of 6,317 feeding lunges (range = 0-12 per dive) were manually
371 identified for those dives when generating true dive summaries from the TDR10 archival data.
372 There was a near-perfect correlation between the two sets of dive summaries for both maximum
373 dive depth and duration (Spearman's rank correlation, $\rho = 1$; Figures A2 and A3 in Additional
374 file). The mean difference in reported maximum dive depth between RDW dives and TDR10
375 dives was 0.57 m (sd = 0.30 m, maximum = 1.4 m), while the mean difference in dive duration
376 was 0.16 min (sd = 0.05 min, maximum = 0.35 min).

377 The threshold values (mean and sd of jerk) of the RDW event detection algorithm stabilized
378 quickly and had no variation after about 80 dives over the initial 13 h of the 17.8-d tracking
379 period (mean jerk = 2/64 G s^{-1}, sd jerk = 4/64 G s^{-1}; Figure A4 in Additional file). The number of
380 detected RDW lunge-feeding events per dive was positively correlated with the number of
381 known feeding lunges detected in the TDR10 archival data (polychoric correlation $r = 0.63$;
382 Figure 2). The mean miss rate by lunges per dive ranged from 0.44 to 0.84 (excluding a single
383 12-lunge dive with a miss rate of 0.08; Figure A5 in Additional file).

384 The per-dive accuracy of the RDW event detection algorithm when classifying feeding/non-
385 feeding dives was 0.74 (binomial proportion 95% CI = 0.73-0.76) when compared to known
386 feeding dives from the TDR10 archival data (Table 1). The true-positive detection rate (i.e., the
387 number of correctly classified feeding dives divided by all known feeding dives) was 0.55,
388 indicating many feeding dives were not accurately identified by the RDW event detection
389 algorithm. However, the false-positive detection rate (i.e., the number of incorrectly classified
390 feeding dives divided by all known feeding dives) was 0.015, indicating that, when a feeding
391 dive was identified, it was almost always correctly classified.

The log-survivorship analysis to identify feeding bouts showed similar trends in relation to the time between feeding dives for both RDW dives and TDR10 dives, although the curve for RDW dives started higher and leveled off more slowly than the curve for TDR10 dives (Figure A6 in Additional file). The probability density distribution of the time between feeding dives showed a high degree of overlap between RDW and TDR10 data (Bhattacharyya's similarity coefficient = 0.82), with most times between feeding dives occurring at ≤ 60 min (Figure A6 in Additional file), indicating a good threshold to differentiate between feeding bouts. Using this threshold, the RDW data generated 70 feeding bouts, 21 of which were single-dive bouts. Since the goal of identifying feeding bouts was to describe feeding activity at broad scales, single-dive bouts were removed, resulting in a total of 49 feeding bouts, compared to 20 true feeding bouts recorded by TDR10 data (none of which were single-dive bouts)

1-mG precision data

Implementing the RDW event detection algorithm at the native (1 mG) resolution of the TDR10 archive data resulted in the detection of 4,452 lunge-feeding events (range = 0-10 per dive; Figure A1 in Additional file) compared to 6,317 known lunge-feeding events in the TDR10 archive. The threshold values (mean and sd of jerk) of the RDW event detection algorithm converged on initial ranges of ± 5 mG s^{-1} after about 110 dives over the initial 19 h of the 17.8-d TDR10 tag deployment, and eventually stabilized to consistent values after approximately one week (mean jerk = 49.9 mG s^{-1}, sd jerk = 67.5 mG s^{-1}; Figure A4 in Additional file). The number of RDW lunge-feeding events per dive detected from 1-mG data was strongly correlated with the number of known feeding lunges from the TDR10 archive data (polychoric correlation $r = 0.88$; Figure 2). The mean miss rate by lunges per dive ranged from 0.10 to 0.31 (Figure A5 in Additional file).

The per-dive accuracy of the RDW event detection algorithm at correctly identifying a feeding dive at the native (1 mG) resolution of the TDR10 archive data was 0.95 (binomial proportion 95% CI = 0.94-0.96) when compared to known feeding dives identified from the TDR10 archive data (Table 1). The true-positive detection rate was 0.96, while the false-positive detection rate was 0.056, indicating that the vast majority of feeding dives were accurately classified by 1-mG RDW dives.

The log-survivorship analysis to identify feeding bouts in the 1-mG data showed very similar trends between RDW dives and TDR10 dives in relation to the time between feeding dives until large times between feeding dives, when the RDW dives reported fewer bouts (Figure A6 in Additional file). The probability density distribution of the time between feeding dives showed a high degree of overlap between RDW and TDR10 dives (Bhattacharyya's similarity coefficient = 0.83), with most times between feeding dives occurring at ≤ 60 min (Figure A6 in Additional file), indicating a good threshold to differentiate between feeding bouts. Using this threshold, the RDW data generated 31 feeding bouts, 11 of which were single-dive bouts. When single-dive bouts were removed, RDW data reported 20 feeding bouts, which was the same recorded by TDR10 data.

Field deployments

Here we present selected case studies to illustrate some applications of the data from RDW tags. The reader is referred to Palacios et al. (58) and Mate et al. (59,60) for complete information about field operations, including the number of tags deployed on each species, year, and region. Individual whales are referred to by the number of the tag they carried (e.g., "whale 1386").

436 *Case study 1: Trends in dive duration in migrating humpback whales tagged in southeastern*
437 *Alaska*

438 For this case study, we compare dive duration and derived metrics for two humpback whales
439 instrumented with RDW-640 tags in southeastern Alaska in November 2015, at the end of the
440 feeding season. These tags reported dive date-times and their durations through Argos for each
441 summarized dive.

442 Whale 1386, a female, was tagged on 17 November near Petersburg and was tracked for 28.3 d
443 and 3,979.6 km before its tag stopped transmitting (Figure 3). Whale 5746, of unknown sex, was
444 tagged on 12 November in Seymour Canal and was tracked for 18.6 d and 1,657.2 km (Figure 3).
445 A total of 213 Argos locations and 1,729 dives were received for whale 1386, while a total of
446 139 Argos locations and 602 dives were received for whale 5746. The proportion of the tracking
447 period summarized by received dives was 25.1% for whale 1386, and 11.1% for whale 5746.
448 The median number of received dives per day was 58 (range: 9-142) for whale 1386 and 30 for
449 whale 5746 (range: 8-77).

450 On average, dive duration, d, was only slightly higher for whale 1386 (mean = 4.08 min, median
451 = 2.80 min, sd = 3.66 min) than for whale 5746 (mean = 3.88 min, median = 2.92 min, sd = 2.95
452 min) ($\log_e(W_{\text{Wilcoxon}}) = 13.12$, p-value = 0.157). In contrast, the post-dive interval, s, was
453 significantly higher for whale 1386 (mean = 1.11 min, median = 0.9 min, sd = 1.07 min) than for
454 whale 5746 (mean = 0.62 min, median = 0.07 min, sd = 1.01 min) ($\log_e(W_{\text{Wilcoxon}}) = 13.44$, p-
455 value < 0.001). The proportion of time spent underwater, U, was significantly lower for whale
456 1386 (mean = 0.8, median = 0.8, sd = 0.16) than for whale 5746 (mean = 0.9, median = 0.97, sd
457 = 0.12) ($\log_e(W_{\text{Wilcoxon}}) = 12.68$, p-value < 0.001). Finally, the ratio of cumulative length of

458 surface interval to cumulative dive duration, r_i, for whale 1386 (mean = 0.27, median = 0.27, sd
459 = 0.02) was twice that of whale 5746 (mean = 0.14, median = 0.14, sd = 0.02) ($\log_e(W_{Wilcoxon})$ =
460 13.85, p-value < 0.001).

461 There was a clear dependence between d and s for the dives received by these two tags, with s
462 increasing with longer d (Figure 3). This dependence was most marked in the range 0-10 min for
463 d and 0-2 min for s. A noticeable difference between the two whales was that whale 1386 made
464 143 dives (8.3%) with d > 10 min (maximum: 24.5 min), while whale 5746 only made 36 dives
465 (6%) with d > 10 min (maximum: 16.6 min) during their respective tracking periods (Figure 3).

466 These two whales had contrasting movement patterns after departing southeastern Alaska, with
467 whale 1386 undertaking an oceanic migration toward the Hawaii breeding area, and whale 5746
468 remaining coastally oriented as it moved southward along British Columbia, Canada (Figure 3).
469 Examination of the temporal variability in dive metrics over the tracking period indicated that
470 whale 5746 generally made short dives with relatively short surface intervals over its 18.6-d
471 tracking period (Figure 4). In contrast, whale 1386 initially made very long dives accompanied
472 by long surface intervals, but once it started migrating, and for the remainder of its 28.3-d
473 tracking period, it made much shorter dives while the surface intervals remained relatively high.
474 Thus, the proportion of time spent underwater for whale 1386 was only occasionally above 0.9,
475 especially in the early part of the tracking period, while it was regularly above 0.9 for whale
476 5746 (Figure 4). These daily trends in d, s, and U were punctuated by sharp departures lasting 1-
477 2 d. In contrast, r_i, because of its cumulative nature, tended to attenuate the strong daily
478 variations over the tracking period. Representing an index of diving capacity, r_i for whale 1386
479 showed an initial decrease but it then leveled off at a relatively high value until the end of the
480 deployment period (Figure 4). In contrast, r_i for whale 5746 was about half the magnitude of that

for whale 1386 and had a more oscillatory behavior over the tracking period, although with an underlying increasing trend (Figure 4).

Case study 2: Changes in blue whale dive behavior over multiple weeks during the feeding season off southern California

For this case study we illustrate changes in dive behavior in relation to space use by an individual blue whale off southern California over the course of the feeding season in summer 2016. Whale 5790, a male, was instrumented with an RDW-665 tag (using version 1 of the event detection algorithm) on 14 July off San Miguel Island and was tracked for 76.4 d and 4,913 km before its tag stopped transmitting (Figure 5). A total of 396 Argos locations and 7,480 dives were received for this whale, with a median of 86 dives reported per day (range: 33-191). The proportion of the tracking duration summarized by received dives was 44%. This field effort used RDW tags programmed with version 1 of the event detection algorithm, which used only an upper threshold to determine periods of high jerk. The number of lunge-feeding events identified per feeding dive (mean = 4.8, sd = 4.2, maximum = 28) was higher than expected (maximum ~ 7 lunges per dive; (20)), leading to the later implementation of version 2 of the algorithm.

For the first 5 d (14-19 July) after tag deployment this whale remained in the area around San Miguel Island, where it fed actively (Figure 6). A marked diel cycle in dive depth and feeding activity was apparent during this period, with dives down to 200 m and a higher number of lunge-feeding events during the day compared to shallow diving and few lunge-feeding events at night. During the following 15 d (20 July - 4 August) the whale largely stopped feeding and the diel cycle in dive depth ceased, with dives mostly limited to < 100 m depth (Figure 6). In this time, the whale left the tagging area and made a clockwise looping excursion to waters south of

San Clemente Island, including spending 8 d over the deeper water of the San Clemente Canyon, before it returned to San Miguel Island (Figure 5). For the final 55 d of the tracking period (5 August - 29 September) the whale remained in the area around San Miguel Island, where the diel cycle resumed and feeding activity was again intense, including dives down to 300 m (Figure 6).

Case study 3: Individual variability in humpback whale feeding behavior off central California

Between 30 July and 4 August 2017, five RDW tags were deployed on humpback whales off Half Moon Bay, central California (Table 2, Figure 7). These RDW tags used version 2 of the event detection algorithm, with both an upper and lower threshold for jerk values. Mean jerk values for these tags ranged from 10/64 to 16/64 G s^{-1}, with values for the two longest-duration tags stabilizing at 11/64 and 12/64 G s^{-1} (whales 833 and 4175, respectively; Table A1 in Additional file). Two of the tagged whales were females and three were males (Table 2). Tracking duration for the five tags ranged from 4.2 to 51.6 d and distances of 216 to 1,535 km. The number of Argos locations received ranged between 33 and 126 and the number of dives between 195 and 2,985. The proportion of track summarized by received dives ranged between 40.3 and 88.7%. The median number of dives per day ranged between 36 and 118 (Table 2).

The five tagged whales ranged between Point Reyes and Monterey Bay during the tracking period (Figure 7), but there was a contrast between the spatial distribution and the intensity of lunge-feeding events for whale 4175 (a female) and the other four whales. Whale 4175 made deeper dives and recorded a higher number of lunge-feeding events per dive when offshore along the continental shelf break and slope, while the other four animals remained over the continental shelf, made shallower dives, and recorded fewer lunge-feeding events per dive (Figures 7 and 8).

Maximum dive depth for whale 4175 was 319 m. Its mean maximum dive depth was two times deeper than the other tagged whales (89.5 versus 45.2 m), and it recorded over three times as many lunge-feeding events compared to the other four tagged whales combined. Lunge-feeding events were most often recorded singularly (mean = 1.1 events per feeding dive) for all tagged whales except whale 4175, which recorded a mean of 2.2 events per feeding dive. A diel cycle was present in the dive data for all animals, with deeper dives and more lunge-feeding events per dive occurring during the day, but it was more marked for whale 4175 (Figure 8). Interestingly, a persistent decrease in deep diving and lunge-feeding event activity appeared to occur in the middle of the day (~ 10:00-14:00 PST), most evident for whale 4175 but also present in the other tagged whales (Figure 8).

Discussion

Proxy validation of dive summary data

The RDW dive summary and event detection algorithms were able to capture with varying success the observed dive and feeding behavior of a blue whale tracked for 17.8 d with a TDR10 tag, whose archival record was used for validation. While maximum dive depth and duration were reported with high accuracy, the number of lunge-feeding events made during a dive had a low accuracy for the 1/64-G precision accelerometer data. However, considering the higher per-dive accuracy and very low false-positive detection rate when classifying dives as feeding or non-feeding, as well as the similarity of feeding bout metrics derived from RDW and TDR10 data, the results were still useful for broad-scale characterization of feeding behavior. Further, the performance of the event detection algorithm was significantly improved in all aspects by increasing the precision of accelerometer readings from 1/64 G to 1 mG.

546 The small mean jerk values calculated from the TDR10 archival data (~ 2/64 G s^{-1}; Figure A4 in
547 Additional file), and used as thresholds to trigger an event detection, meant that the minimum
548 jerk criteria (less than half the mean jerk) could not be resolved well at 1/64-G resolution. The
549 added precision of the 1-mG data better resolved these small values, allowing for a greater
550 number of possible values that met the minimum jerk criteria, resulting in improved detection
551 performance. All new versions of the RDW tag now support 1-mG precision accelerometer data.
552 Parenthetically, the RDW event detection algorithm at the 1/64-G precision may have performed
553 better during field deployments than our validation results indicated for instances when mean
554 and sd jerk threshold values were larger than those reported for the TDR10 data, as was observed
555 for the field deployments in case study 3, which ranged from 10/64 to 16/64 G s^{-1}.

556 Log-survivorship curves to identify feeding bouts from the time between feeding dives were
557 generally similar in shape for both 1/64- and 1-mG data, although the 1/64-G data produced
558 higher numbers of bouts at short non-feeding dive intervals. This discrepancy was likely due to
559 the high number of false-negative feeding dives identified by the RDW event detection
560 algorithm, which divided feeding bouts observed in the continuous TDR10 archival data into
561 multiple shorter bouts. An implementation of this feeding bout analysis is not currently feasible
562 for field deployments of RDW tags, as limitations of satellite coverage, whale surfacing
563 behavior, and other factors affecting tag transmission can result in often incomplete time series
564 of dive summaries (e.g., Figure 6). However, planned improvements to the Argos satellite
565 constellation, as well as other recent developments to improve reception of satellite
566 transmissions (62,63) raise the possibility of better data recovery in the future, leading to an
567 improved ability to characterize feeding behavior over broader spatial and temporal scales.

568 **Field deployments**

569 The two humpback whales instrumented in southeastern Alaska in 2015 revealed marked inter-
570 individual differences in their dive time budget while in the southeastern Alaska feeding area,
571 despite having been tagged in relatively close proximity. After the two animals left the area, the
572 temporal pattern in dive behavior for whale 1386 likely reflected the dive time budget of an
573 animal engaged in directed, open-ocean migration toward the Hawaii breeding area, while the
574 high proportion of time spent underwater for whale 5746 suggested that it continued to engage in
575 coastal foraging as it moved down the coast of British Columbia. The ability of these tags to
576 report dive duration for extended periods of time provided an opportunity to study a running
577 index of dive capacity (the ratio r_i), with implications for monitoring trends in dive physiology
578 and performance beyond local-scale studies (64–68).

579 An RDW tag attached to a blue whale off southern California in 2016 showed dramatic shifts in
580 dive depth and feeding behavior over its 76-d tracking period, including an extended period of
581 interrupted feeding between two periods of intense feeding. While the number of lunge-feeding
582 events recorded were higher than expected with version 1 of the event detection algorithm, the
583 overall trend of behavior followed well-known patterns of blue whale feeding (22,42). Most
584 studies using short-duration tags have shown intense feeding by blue whales in southern
585 California (19,20,69–71), but only recently are we starting to learn about the extent of variability
586 in feeding effort and prey patchiness when examined over longer periods of time and at a more
587 regional scales using medium-duration archival tags (22,24).

588 An improved understanding of these changes in behavioral state through the use of RDW tags
589 has relevance to studies assessing whale responses to acoustic disturbance such as from Navy
590 sonar. Studies of exposure to acoustic disturbance in areas of high prey density have shown that
591 blue whales are less likely to initiate deep foraging behavior, or they may move away from high-

592 quality prey patches at depth when loud sound sources are active (25,26,72). However, careful
593 consideration of the baseline behavioral context prior to the experiment is needed, especially to
594 recognize longer-term effects. The ability of RDW tags to monitor large whale behavior for
595 periods of months offers a new tool to begin addressing these issues over broader time scales.

596 The case study with RDW-tagged humpback whales off central California in 2017 demonstrated
597 that striking differences in dive behavior, feeding activity, and habitat use between individuals
598 can occur over small spatial scales. The contrast in dive depth and lunge-feeding intensity
599 between the four inner-shelf-associated whales and the whale that primarily foraged along the
600 adjacent shelf break and continental slope (whale 4175), was evidence that these two groups of
601 animals may have been exploiting different prey resources. Off central California, humpback
602 whales and other marine predators are known to switch their dominant prey between euphausiids
603 and schooling fish in response to changing climatic conditions (73,74). While these shifts
604 primarily occur over time, the spatial heterogeneity in oceanographic conditions and the
605 complexity of the bottom topography of this region also result in contemporaneous habitats
606 favorable for schooling fish over the inner shelf and for krill over the shelf break (75,76), which
607 may vary on a scale of days (77). Thus, we speculate that whale 4175 may have been primarily
608 feeding on euphausiids while the other four whales may have been primarily feeding on
609 schooling fish. If our speculation is correct, the individual variability in the number of lunge-
610 feeding events per dive would further suggest that humpback whales can have distinct foraging
611 strategies to exploit different prey resources at fairly local scales.

612 Indeed, the two groups of whales were not completely segregated during the tracking period, as
613 at least one shelf-associated animal also fed over the shelf break in the same area used by whale
614 4175 (Figure 7). Clusters of deeper dives and higher numbers of lunge-feeding events by shelf-

associated whales (Figure 8) may indicate a shift in foraging strategy during brief use of the shelf-break habitat. In this central California ecosystem, humpback whales are known to seasonally shift their prey from euphausiids in spring to schooling fish later in summer, when blue whales (a euphausiid specialist) arrive (78). These humpback whales are thought to exploit their more generalist diet by switching target prey species based on their relative abundance (78) and our results suggest this may happen on relatively short time scales. Alternatively, social dynamics may drive the variability in foraging behavior we observed off central California, similar to how humpback whales in a British Columbia feeding area are more commonly associated with others employing the same feeding strategies (79).

Limitations

Recovery of data from instrumented animals is a significant hurdle for research, especially when conducted on large whales, which can move > 100 km per day and do not return to a central place where a tag can reliably be recovered (3,80). For RDW tags, data recovery is limited by the coincident occurrence of the tagged whale surfacing while an Argos satellite is overhead to receive a transmission. The duration of recorded dives can also affect data recovery, as longer dives will summarize a greater portion of the tracking period with each transmission. Collectively, this means that dive summary time series from RDW tags are rarely complete, and the number of dives reported from each tag can vary widely depending on individual behavior. Extrinsic factors like bad weather or biofouling can also affect data recovery by limiting satellite transmissions. The biases associated with these irregular dive summaries are related to the degree of irregularity and the scale of the behavior being studied (81,82), but a more adequate characterization will require dedicated research. For these reasons, RDW tags should be

637 considered to provide a relative index of dive behavior, rather than a continuous and complete
638 record.

639 We assumed that the received dives were a random sample of selected dives that occurred during
640 the tracking period. However, the process of grouping consecutive dives for transmission may
641 introduce bias through serial correlation, while the whales' surfacing patterns and tag duty
642 cycling may further contribute to a lack of independence in ways that remain to be characterized.
643 Thus, more research is needed to assess how dive summaries are received, if animal behavior
644 might affect these trends, and how the relevant scales of behavior being studied might be
645 affected. For this reason, *in-situ* validation of detected events by means of using concurrently
646 attached data loggers on whales carrying RDW tags remains a high priority.

647 ## Conclusions

648 The correspondence between RDW and TDR10 dive summaries and their derived feeding bouts
649 in the proxy validation exercise demonstrated that RDW tags can link local-scale behavior to
650 broader, ecosystem-scale processes by monitoring per-dive behavior over multi-month
651 timescales of movement. A previous study using medium-duration tags (22) showed that the
652 number of feeding lunges made per dive is related to the duration of feeding bouts in both blue
653 and fin whales, suggesting that longer-term behavioral monitoring can more fully describe the
654 drivers of residence time over the course of the feeding season. Indeed, the data on temporal and
655 spatial variability of local-scale behavior derived from RDW tags presented in this study offered
656 insight into the characteristics of whale foraging behavior at broader scales, which in turn could
657 reveal new information on strategies of individual feeding specialization and inter-specific
658 habitat partitioning. Additionally, these behaviorally mediated processes can lead to variable or

659 differential exposure to anthropogenic impacts (22,24,83), making this information highly useful
660 to management and conservation organizations.

661 Conceptually, the flexible sensor configuration and adaptive software capabilities of RDW tags
662 makes them generalizable for a variety of applications with cetaceans, which may extend to
663 studies of species that use other foraging tactics like raptorial feeding or ram-filtration (84).
664 Known behavioral cues associated with non-feeding behaviors could also be incorporated into
665 the event detection algorithm, for example to investigate patterns and trends in male singing
666 (85,86) or agonistic interactions (87). The tags could also be used to monitor changes in body
667 condition over time based on trends in buoyancy, as implemented through hydrodynamic glide
668 models (88–90). Such information would further inform studies of the effects of anthropogenic
669 disturbance on individuals and how related changes in fitness might scale up to the larger
670 population (e.g., (91,92)).

671 Advances in microprocessor technology continue to reduce component size, operating voltage,
672 and current consumption, while at the same time increasing the available on-board memory and
673 processing speed. Future improvements to the software (e.g., refinement of event detection
674 algorithms) and advances in hardware (e.g., addition of other environmental sensors and
675 increasing sensor precision) will further expand RDW tag applications for ecology, management,
676 and conservation. The RDW tag joins a new generation of devices with the technological
677 capacity to collect and, in some cases, process large volumes of data onboard (24,38,93). These
678 advances pave the way for the routine generation of key metrics of dive behavior for marine
679 wildlife onboard non-recoverable smart tags across large spatial and temporal scales, while the
680 ability to dynamically update event detection parameters (e.g., to account for differences in tag

placement or behavioral trends) offers opportunities for improved long-term behavioral and physiological monitoring.

List of abbreviations

SWS: saltwater conductivity switch

NMFS: U.S. National Marine Fisheries Service

Declarations

Ethics approval

The activities reported in this study involving deployment of RDW tags on large whales were carried out under the authorization of U.S. National Marine Fisheries Service (NMFS) Marine Mammal Protection Act and Endangered Species Act scientific research permit No. 14856 and Oregon State University Institutional Animal Care and Use Committee Permit Nos. 4495 and 4884, issued to Bruce R Mate. The activities involving deployment of the TDR10-F archival tag on large whales were carried out under NMFS permit No. 16111-02 issued to John Calambokidis.

Consent for publication

Not applicable.

Availability of data and materials

698 The datasets supporting the conclusions of this article, including the 4-Hz, 1/64-G TDR10 data,
699 will be deposited in a Movebank Repository (https://www.datarepository.movebank.org) upon
700 acceptance.

701 **Competing interests**

702 ST is Director of Telonics, Inc., which developed the RDW tags for commercial use. As the
703 manufacturer, Telonics may benefit from the publication of this manuscript.

704 **Funding**

705 Funding for tagging humpback whales in southeastern Alaska in 2015 was provided by a grant
706 from Pacific Life Foundation. Blue whale tagging in southern California in 2016 was supported
707 by the U.S. Department of the Navy, Commander, Pacific Fleet under the Marine Species
708 Monitoring Program via contract with HDR, Inc. (Contract No. N62470-15-D-8006). Humpback
709 whale tagging off central California in 2017 was supported by Commander, Pacific Fleet, and
710 Commander, Naval Sea Systems Command, through a Cooperative Ecosystem Studies Unit
711 (CESU) agreement (Cooperative Agreement No. N62473-17-2-0001). Both projects were
712 administered by Naval Facilities Engineering Command (NAVFAC) Southwest. We thank
713 Andrea Balla-Holden and Chip Johnson for serving as Representatives for Commander, Pacific
714 Fleet, and Commander, Naval Sea Systems Command, respectively. Jessica Bredvik and Reagan
715 Pablo at NAVFAC served as the Technical Representative and the Agreement Administrator of
716 these awards, respectively. We also thank Kristen Ampela at HDR, Inc. for project management.
717 Activities conducted by Cascadia Research Collective reported in this paper were funded in part
718 by the U.S. Office of Naval Research and NMFS.

Author's contributions

DP and LI conceived the conceptual approach of the manuscript. ST led the design and development of the RDW devices for Telonics, Inc. LI contributed to the development of event detection algorithms. LI and BL conducted the testing of sensor functionality in the lab and contributed to the RDW field data collection. JF and JC collected the TDR10 data, analyzed the TDR10 record, and contributed to RDW validation. DP and LI analyzed the data. DP drafted the manuscript with contributions from LI, BL, ST, and BM. All authors read and approved the final manuscript.

Acknowledgements

We thank Telonics engineers Jeff Tenney and Chris Lusko for their invaluable support in the technical development and validation of the RDW tags. We gratefully acknowledge the support in the field provided by Captain Dennis Rogers and the crew of the M/V *Northern Song* in Alaska, and by Captain Ron Briggs and the crew of the R/V *Pacific Storm* in California. We also thank the people who assisted with tagging operations, including Ken Serven, Martha Winsor, Craig Hayslip, Tomas Follett, Kris Bauer, Steve Lewis, Will Sheehy, Kyle Milliken, and Colin Gillin. At the Oregon State University Marine Mammal Institute, we acknowledge C. Scott Baker and Debbie Steel of the Cetacean Conservation and Genomics Laboratory for genetic sex determination of biopsy samples of tagged whales; Tomas Follett for database management; and Kathy Minta, Mark Wilke, and Minda Stiles for logistical and administrative support. We also thank Beto Alvarez for drafting Figure 1.

The Argos Data Collection and Location System was used for this project (http://www.argos-system.org/). The system is operated by Collecte Localisation Satellites. Argos is an international

741 program that relies on instruments provided by the French Space Agency flown on polar-orbiting
742 satellites operated by the U.S. National Oceanic and Atmospheric Administration, the European
743 Organisation for the Exploitation of Meteorological Satellites, and the Indian Space Research
744 Organization.

745 # References

746 1. Kays R, Crofoot MC, Jetz W, Wikelski M. Terrestrial animal tracking as an eye on life and
747 planet. Science. 2015;348(6240).

748 2. Hussey NE, Kessel ST, Aarestrup K, Cooke SJ, Cowley PD, Fisk AT, et al. Aquatic animal
749 telemetry: A panoramic window into the underwater world. Science. 2015;348(6240).

750 3. Mate B, Mesecar R, Lagerquist B. The evolution of satellite-monitored radio tags for large
751 whales: One laboratory's experience. Deep Sea Research Part II: Topical Studies in
752 Oceanography. 2007;54(3):224–47.

753 4. Andrews RD, Baird RW, Calambokidis J, Goertz CEC, Gulland FMD, Heide-Jørgensen MP, et
754 al. Best practice guidelines for cetacean tagging. Journal of Cetacean Research and
755 Management. 2019;20:27–66.

756 5. Heide-Jørgensen MP, Kleivane L, ØIen N, Laidre KL, Jensen MV. A new technique for
757 deploying satellite transmitters on baleen whales: Tracking a blue whale (*Balaenoptera*
758 *musculus*) in the North Atlantic. Marine Mammal Science. 2001;17(4):949–54.

759 6. Zerbini AN, Andriolo A, Heide-Jørgensen MP, Pizzorno JL, Maia YG, VanBlaricom GR, et al.
760 Satellite-monitored movements of humpback whales *Megaptera novaeangliae* in the
761 Southwest Atlantic Ocean. Marine Ecology Progress Series. 2006;313:295–304.

762 7. Citta JJ, Quakenbush LT, Okkonen SR, Druckenmiller ML, Maslowski W, Clement-Kinney J, et
763 al. Ecological characteristics of core-use areas used by Bering–Chukchi–Beaufort (BCB)
764 bowhead whales, 2006–2012. Progress in Oceanography. August;136:201–22.

765 8. Weinstein BG, Irvine L, Friedlaender AS. Capturing foraging and resting behavior using
766 nested multivariate Markov models in an air-breathing marine vertebrate. Movement
767 Ecology. 2018;6(1):16.

768 9. Derville S, Torres LG, Zerbini AN, Oremus M, Garrigue C. Horizontal and vertical movements
769 of humpback whales inform the use of critical pelagic habitats in the western South Pacific.
770 Scientific Reports. 2020;10(1):1–13.

10. Lagerquist BA, Mate BR, Ortega-Ortiz JG, Winsor M, Urbán-Ramirez J. Migratory movements and surfacing rates of humpback whales (*Megaptera novaeangliae*) satellite tagged at Socorro Island, Mexico. Marine Mammal Science. 2008;24(4):815–30.

11. Chambault P, Fossette S, Heide-Jørgensen MP, Jouannet D, Vély M. Predicting seasonal movements and distribution of the sperm whale using machine learning algorithms. Ecology and Evolution. 2021;11(3):1432–45.

12. Miller PJO, Johnson MP, Tyack PL. Sperm whale behaviour indicates the use of echolocation click buzzes 'creaks' in prey capture. Proceedings of the Royal Society of London Series B: Biological Sciences. 2004;271(1554):2239–47.

13. Allen AN, Goldbogen JA, Friedlaender AS, Calambokidis J. Development of an automated method of detecting stereotyped feeding events in multisensor data from tagged rorqual whales. Ecology and Evolution. 2016;6(20):7522–35.

14. Sweeney DA, DeRuiter SL, McNamara-Oh YJ, Marques TA, Arranz P, Calambokidis J. Automated peak detection method for behavioral event identification: detecting *Balaenoptera musculus* and *Grampus griseus* feeding attempts. Animal Biotelemetry. 2019;7(1):7.

15. Goldbogen JA, Cade DE, Calambokidis J, Friedlaender AS, Potvin J, Segre PS, et al. How baleen whales feed: The biomechanics of engulfment and filtration. Annual Review of Marine Science. 2017;9(1):367–86.

16. Simon M, Johnson M, Madsen PT. Keeping momentum with a mouthful of water: behavior and kinematics of humpback whale lunge feeding. Journal of Experimental Biology. 2012;215(21):3786–98.

17. Goldbogen JA, Cade DE, Boersma AT, Calambokidis J, Kahane-Rapport SR, Segre PS, et al. Using digital tags with integrated video and inertial sensors to study moving morphology and associated function in large aquatic vertebrates. The Anatomical Record. 2017;300(11):1935–41.

18. Owen K, Dunlop RA, Monty JP, Chung D, Noad MJ, Donnelly D, et al. Detecting surface-feeding behavior by rorqual whales in accelerometer data. Marine Mammal Science. 2016;32(1):327–48.

19. Goldbogen JA, Hazen EL, Friedlaender AS, Calambokidis J, DeRuiter SL, Stimpert AK, et al. Prey density and distribution drive the three-dimensional foraging strategies of the largest filter feeder. Functional Ecology. 2015;29(7):951–61.

20. Hazen EL, Friedlaender AS, Goldbogen JA. Blue whales (*Balaenoptera musculus*) optimize foraging efficiency by balancing oxygen use and energy gain as a function of prey density. Science Advances. 2015;1(9):e1500469.

21. Cade DE, Seakamela SM, Findlay KP, Fukunaga J, Kahane-Rapport SR, Warren JD, et al. Predator-scale spatial analysis of intra-patch prey distribution reveals the energetic drivers of rorqual whale super-group formation. Functional Ecology. 2021;35(4):894–908.

22. Irvine LM, Palacios DM, Lagerquist BA, Mate BR. Scales of blue and fin whale feeding behavior off California, USA, with implications for prey patchiness. Frontiers in Ecology and Evolution. 2019;7.

23. Irvine L, Palacios DM, Urbán J, Mate B. Sperm whale dive behavior characteristics derived from intermediate-duration archival tag data. Ecology and Evolution. 2017;7(19):7822–37.

24. Calambokidis J, Fahlbusch JA, Szesciorka AR, Southall BL, Cade DE, Friedlaender AS, et al. Differential vulnerability to ship strikes between day and night for blue, fin, and humpback whales based on dive and movement data from medium duration archival tags. Frontiers in Marine Science. 2019;6.

25. DeRuiter SL, Langrock R, Skirbutas T, Goldbogen JA, Calambokidis J, Friedlaender AS, et al. A multivariate mixed hidden Markov model for blue whale behaviour and responses to sound exposure. Annals of Applied Statistics. 2017;11(1):362–92.

26. Goldbogen JA, Southall BL, DeRuiter SL, Calambokidis J, Friedlaender AS, Hazen EL, et al. Blue whales respond to simulated mid-frequency military sonar. Proceedings of the Royal Society B: Biological Sciences. 2013;280(1765):20130657.

27. Owen K, Jenner CS, Jenner M-NM, Andrews RD. A week in the life of a pygmy blue whale: migratory dive depth overlaps with large vessel drafts. Animal Biotelemetry. 2016;4(1):17.

28. Johnson MP, Tyack PL. A digital acoustic recording tag for measuring the response of wild marine mammals to sound. IEEE Journal of Oceanic Engineering. 2003;28(1):3–12.

29. Mate BR, Irvine LM, Palacios DM. The development of an intermediate-duration tag to characterize the diving behavior of large whales. Ecology and Evolution. 2017;7(2):585–95.

30. Szesciorka AR, Calambokidis J, Harvey JT. Testing tag attachments to increase the attachment duration of archival tags on baleen whales. Animal Biotelemetry. 2016;4(1):18.

31. Baumgartner MF, Hammar T, Robbins J. Development and assessment of a new dermal attachment for short-term tagging studies of baleen whales. Methods in Ecology and Evolution. 2015;6(3):289–97.

32. Bailey H, Mate BR, Palacios DM, Irvine L, Bograd SJ, Costa DP. Behavioural estimation of blue whale movements in the Northeast Pacific from state-space model analysis of satellite tracks. Endangered Species Research. 2009;10:93–106.

838 33. Palacios DM, Bailey H, Becker EA, Bograd SJ, DeAngelis ML, Forney KA, et al. Ecological
839 correlates of blue whale movement behavior and its predictability in the California Current
840 Ecosystem during the summer-fall feeding season. Movement Ecology. 2019;7(1):26.

841 34. Johnson DH. The comparison of usage and availability measurements for evaluating
842 resource preference. Ecology. 1980;61(1):65–71.

843 35. Abrahms B, Aikens EO, Armstrong JB, Deacy WW, Kauffman MJ, Merkle JA. Emerging
844 perspectives on resource tracking and animal movement ecology. Trends in Ecology &
845 Evolution. 2020;36(4):308–20.

846 36. Tomkiewicz MSM. Development of intelligent PTTs with emphasis on sensor technology
847 applicable to wildlife research programs. Pages 97-104 in Parc national du Mercantour,
848 "Suivi par radiotélémétrie des vertébrés terrestres," Actes du Colloque International,
849 Monaco, 12 - 13 décembre 1988.; 1989. Available from:
850 https://documentation.ensg.eu/index.php?lvl=notice_display&id=35287

851 37. Heerah K, Hindell M, Guinet C, Charrassin J-B. From high-resolution to low-resolution dive
852 datasets: a new index to quantify the foraging effort of marine predators. Animal
853 Biotelemetry. 2015;3(1):42.

854 38. Skubel RA, Wilson K, Papastamatiou YP, Verkamp HJ, Sulikowski JA, Benetti D, et al. A
855 scalable, satellite-transmitted data product for monitoring high-activity events in mobile
856 aquatic animals. Animal Biotelemetry. 2020;8(1):34.

857 39. Pohlot BG, Ehrhardt N. An analysis of sailfish daily activity in the Eastern Pacific Ocean using
858 satellite tagging and recreational fisheries data. ICES Journal of Marine Science.
859 2018;75(2):871–9.

860 40. Martín López LM, Miller PJO, Aguilar de Soto N, Johnson M. Gait switches in deep-diving
861 beaked whales: biomechanical strategies for long-duration dives. Journal of Experimental
862 Biology. 2015;218(9):1325–38.

863 41. Wilson RP, Börger L, Holton MD, Scantlebury DM, Gómez-Laich A, Quintana F, et al.
864 Estimates for energy expenditure in free-living animals using acceleration proxies: A
865 reappraisal. Journal of Animal Ecology. 2020;89(1):161–72.

866 42. Calambokidis J, Schorr GS, Steiger GH, Francis J, Bakhtiari M, Marshall G, et al. Insights into
867 the underwater diving, feeding, and calling behavior of blue whales from a suction-cup-
868 attached video-imaging tag (Crittercam). Marine Technology Society; 2007.

869 43. Goldbogen JA, Calambokidis J, Croll DA, Harvey JT, Newton KM, Oleson EM, et al. Foraging
870 behavior of humpback whales: kinematic and respiratory patterns suggest a high cost for a
871 lunge. Journal of Experimental Biology. 2008;211(23):3712–9.

44. Core Team R. R: A language and environment for statistical computing.. R Foundation for statistical computing. Vienna, Austria.; 2020. Available from: https://www.R-project.org/.

45. Cade DE, Friedlaender AS, Calambokidis J, Goldbogen JA. Kinematic diversity in rorqual whale feeding mechanisms. Current Biology. 2016;26(19):2617–24.

46. Fox J. polycor: Polychoric and Polyserial Correlations. R package version 0.7-10.; 2019. Available from: https://CRAN.R-project.org/package=polycor.

47. Torres LG. A sense of scale: Foraging cetaceans' use of scale-dependent multimodal sensory systems. Marine Mammal Science. 2017;33(4):1170–93.

48. Kuhn M, Wing J, Weston S, Williams A, Keefer C, Englehardt A, et al. caret: Classification and Regression Training. R package version 6.0-84; 2019. Available from: https://CRAN.R-project.org/package=caret

49. Holford TR. The analysis of rates and of survivorship using log-linear models. Biometrics. 1980;36(2):299–305.

50. Gentry RL, Kooyman GL. Fur Seals. Princeton, NJ: Princeton University Press; 1986. 312 p.

51. Guillerme T, Cooper N. Effects of missing data on topological inference using a Total Evidence approach. Molecular Phylogenetics and Evolution. 2016;94:146–58.

52. Bhattacharyya A. On a measure of divergence between two statistical populations defined by their probability distributions. Bulletin of the Calcutta Mathematical Society. 1943;35:99–109.

53. Noren DP, Mocklin JA. Review of cetacean biopsy techniques: Factors contributing to successful sample collection and physiological and behavioral impacts. Marine Mammal Science. 2012;28(1):154–99.

54. Aasen E, Medrano JF. Amplification of the Zfy and Zfx genes for sex identification in humans, cattle, sheep and goats. Nature Biotechnology. 1990;8(12):1279–81.

55. Gilson A, Syvanen M, Levine K, Banks J. Deer gender determination by polymerase chain reaction: Validation study and application to tissues, bloodstains, and hair forensic samples from California. California Fish & Game. 1998;84(4):159–69.

56. Katona SK, Whitehead HP. Identifying humpback whales using their natural markings. Polar Record. 1981;20(128):439–44.

57. Gendron D, Ugalde De La Cruz A. A new classification method to simplify blue whale photo-identification technique. Journal of Cetacean Research and Management. 2012;12(1):6.

58. Palacios D, Mate BR, Baker CS, Lagerquist B, Irvine LM, Follett TM, et al. Humpback Whale Tagging in Support of Marine Mammal Monitoring Across Multiple Navy Training Areas in the Pacific Ocean: Final Report for the Hawaiian Breeding Area in Spring 2019, Including Historical Data from Previous Tagging Efforts. Prepared for Commander, US Pacific Fleet, and Commander, Naval Sea Systems Command. Submitted to Naval Facilities Engineering Command Southwest, San Diego, California, under Cooperative Ecosystem Studies Unit, Department of the Navy Cooperative Agreement No. N62473-17-2-0001; 2020.

59. Mate BR, Palacios DM, Baker CS, Lagerquist BA, Irvine LM, Follett T, et al. Baleen Whale Tagging in Support of Marine Mammal Monitoring Across Multiple Navy Training Areas Covering the Years 2014, 2015, 2016, and 2017. 2018 p. 180. (Prepared for Commander, U.S. Pacific Fleet. Submitted to Naval Facilities Engineering Command Southwest under Contract No. N62470-15-8006-17F4016 issued to HDR, Inc., San Diego, California.). Available from: https://www.navymarinespeciesmonitoring.us/files/2415/5484/0267/Mate_et_al_2018_Baleen_Whale_Tagging_on_US_West_Coast.pdf

60. Mate BR, Palacios DM, Baker CS, Irvine LM, Lagerquist BA, Follett TM, et al. Humpback Whale Tagging in Support of Marine Mammal Monitoring Across Multiple Navy Training Areas in the Pacific Ocean. 2018 p. 160. (Final Report for Feeding Areas off the US West Coast in Summer-Fall 2017, Including Historical Data from Previous Tagging Efforts. Prepared for Commander, US Pacific Fleet and Commander, Naval Sea Systems Command. Submitted to Naval Facilities Engineering Command Southwest, San Diego, California, under Cooperative Ecosystem Studies Unit, Department of the Navy Cooperative Agreement No. N62473-17-2-0001.). Available from: https://www.navymarinespeciesmonitoring.us/files/1915/5484/0269/Mate_et_al_2018_Humpback_Whale_Tagging_on_US_West_Coast_Summer-Fall_2017.pdf

61. Irvine LM, Winsor MH, Follett TM, Mate BR, Palacios DM. An at-sea assessment of Argos location accuracy for three species of large whales, and the effect of deep-diving behavior on location error. Animal Biotelemetry. 2020;8(1):20.

62. Jeanniard-du-Dot T, Holland K, Schorr GS, Vo D. Motes enhance data recovery from satellite-relayed biologgers and can facilitate collaborative research into marine habitat utilization. Animal Biotelemetry. 2017;5(1):17.

63. Billie M, Dendiu R, Baker L, Brune S, Byrnes I, Round C. Microsats and moby dick: microsatellite support to whale science and conservation. In: Proceedings, 32nd Annual AIAA/USU Conference on Small Satellites. Paper number SSC18-V-07. 1-11.; 2018.

64. Keen EM, Qualls KM. Respiratory behaviors in sympatric rorqual whales: the influence of prey depth and implications for temporal access to prey. Journal of Mammalogy. 2018;99(1):27–40.

65. Dolphin WF. Ventilation and dive patterns of humpback whales, *Megaptera novaeangliae*, on their Alaskan feeding grounds. Canadian Journal of Zoology. 1987;65(1):83–90.

66. Dolphin WF. Foraging dive patterns of humpback whales, *Megaptera novaeangliae*, in southeast Alaska: a cost–benefit analysis. Canadian Journal of Zoology. 1988;66(11):2432–41.

67. Williams HJ, Shipley JR, Rutz C, Wikelski M, Wilkes M, Hawkes LA. Future trends in measuring physiology in free-living animals. Philosophical Transactions of the Royal Society B: Biological Sciences. 2021;376(1831):20200230.

68. Watanabe YY, Goldbogen JA. Too big to study? The biologging approach to understanding the behavioural energetics of ocean giants. Journal of Experimental Biology. 2021;224(13).

69. Acevedo-Gutiérrez A, Croll DA, Tershy BR. High feeding costs limit dive time in the largest whales. Journal of Experimental Biology. 2002;205(12):1747–53.

70. Croll DA, Tershy BR, Hewitt RP, Demer DA, Fiedler PC, Smith SE, et al. An integrated approach to the foraging ecology of marine birds and mammals. Deep Sea Research Part II: Topical Studies in Oceanography. 1998;45(7):1353–71.

71. Friedlaender AS, Goldbogen JA, Hazen EL, Calambokidis J, Southall BL. Feeding performance by sympatric blue and fin whales exploiting a common prey resource. Marine Mammal Science. 2015;31(1):345–54.

72. Friedlaender AS, Johnston DW, Tyson RB, Kaltenberg A, Goldbogen JA, Stimpert AK, et al. Multiple-stage decisions in a marine central-place forager. Royal Society Open Science. 2016;3(5):160043.

73. Fleming AH, Clark CT, Calambokidis J, Barlow J. Humpback whale diets respond to variance in ocean climate and ecosystem conditions in the California Current. Global Change Biology. 2016;22(3):1214–24.

74. Warzybok P, Santora JA, Ainley DG, Bradley RW, Field JC, Capitolo PJ, et al. Prey switching and consumption by seabirds in the central California Current upwelling ecosystem: Implications for forage fish management. Journal of Marine Systems. 2018;185:25–39.

75. Santora JA, Sydeman WJ, Schroeder ID, Wells BK, Field JC. Mesoscale structure and oceanographic determinants of krill hotspots in the California Current: Implications for trophic transfer and conservation. Progress in Oceanography. 2011;91(4):397–409.

76. Santora JA, Sydeman WJ, Schroeder ID, Reiss CS, Wells BK, Field JC, et al. Krill space: a comparative assessment of mesoscale structuring in polar and temperate marine ecosystems. ICES Journal of Marine Science. 2012;69(7):1317–27.

77. Benoit-Bird KJ, Waluk CM, Ryan JP. Forage species swarm in response to coastal upwelling. Geophysical Research Letters. 2019;46(3):1537–46.

78. Fossette S, Abrahms B, Hazen EL, Bograd SJ, Zilliacus KM, Calambokidis J, et al. Resource partitioning facilitates coexistence in sympatric cetaceans in the California Current. Ecology and Evolution. 2017;7(21):9085–97.

79. Wray J, Keen E, O'Mahony ÉN. Social survival: Humpback whales (*Megaptera novaeangliae*) use social structure to partition ecological niches within proposed critical habitat. PLOS ONE. 2021;16(6):e0245409.

80. Mate BR, Lagerquist BA, Calambokidis J. Movements of North Pacific blue whales during the feeding season off southern California and their southern fall migration. Marine Mammal Science. 1999;15(4):1246–57.

81. Mul E, Blanchet M-A, Biuw M, Rikardsen A. Implications of tag positioning and performance on the analysis of cetacean movement. Animal Biotelemetry. 2019;7(1):11.

82. Breed GA, Costa DP, Goebel ME, Robinson PW. Electronic tracking tag programming is critical to data collection for behavioral time-series analysis. Ecosphere. 2011;2(1):art10.

83. Keen EM, Falcone EA, Andrews RD, Schorr GS. Diel Dive Behavior of Fin Whales (*Balaenoptera physalus*) in the Southern California Bight. Aquatic Mammals. 2019;45(2):233–43.

84. Heithaus MR, Dill LM, Kiszka JJ. Feeding strategies and tactics. In: Wursig B, Thewissen JGM, Kovacs KM, editors. Encyclopedia of Marine Mammals - 3rd Edition. Cambridge, MA, USA: Academic Press; 2018. p. 354–63.

85. Oestreich WK, Fahlbusch JA, Cade DE, Calambokidis J, Margolina T, Joseph J, et al. Animal-borne metrics enable acoustic detection of blue whale migration. Current Biology. 2020;30(23):4773-4779.e3.

86. Stimpert AK, DeRuiter SL, Falcone EA, Joseph J, Douglas AB, Moretti DJ, et al. Sound production and associated behavior of tagged fin whales (*Balaenoptera physalus*) in the Southern California Bight. Animal Biotelemetry. 2015;3(1):23.

87. Baker CS, Herman LM. Aggressive behavior between humpback whales (*Megaptera novaeangliae*) wintering in Hawaiian waters. Canadian Journal of Zoology. 1984;62(10):1922–37.

88. Aoki K, Isojunno S, Bellot C, Iwata T, Kershaw J, Akiyama Y, et al. Aerial photogrammetry and tag-derived tissue density reveal patterns of lipid-store body condition of humpback whales on their feeding grounds. Proceedings of the Royal Society B: Biological Sciences. 2021;288(1943):20202307.

89. Miller P, Narazaki T, Isojunno S, Aoki K, Smout S, Sato K. Body density and diving gas volume of the northern bottlenose whale (*Hyperoodon ampullatus*). Journal of Experimental Biology. 2016;219(16):2458–68.

90. Narazaki T, Isojunno S, Nowacek DP, Swift R, Friedlaender AS, Ramp C, et al. Body density of humpback whales (*Megaptera novaengliae*) in feeding aggregations estimated from hydrodynamic gliding performance. PLOS ONE. 2018;13(7):e0200287.

91. Pirotta E, Schwarz LK, Costa DP, Robinson PW, New L. Modeling the functional link between movement, feeding activity, and condition in a marine predator. Behavioral Ecology. 2019;30(2):434–45.

92. Pirotta E, Booth CG, Cade DE, Calambokidis J, Costa DP, Fahlbusch JA, et al. Context-dependent variability in the predicted daily energetic costs of disturbance for blue whales. Conservation Physiology. 2021;9(1):coaa137.

93. Cox SL, Orgeret F, Gesta M, Rodde C, Heizer I, Weimerskirch H, et al. Processing of acceleration and dive data on-board satellite relay tags to investigate diving and foraging behaviour in free-ranging marine predators. Methods in Ecology and Evolution. 2018;9(1):64–77.

Additional files

additional_file.pdf

Title: Additional file: Additional table and figures

Description: This file contains one table and six additional figures providing supplementary information related to the proxy validation of the RDW tag dive summary and event detection algorithms.

Table 1. Confusion matrix showing the classification of feeding and non-feeding dives by version 2 of the RDW-665 event detection algorithm compared to dives summarized from continuous Wildlife Computers TDR10-F archive data.

		TDR10 archive dives	
		Feeding	Non-feeding
1/64-G RDW dives	Feeding	733	20
	Non-feeding	612	1,097
1-mG RDW dives	Feeding	1,297	75
	Non-feeding	48	1,042

Table 2. Summary of location and dive data collected by five RDW tags deployed on humpback whales off central California during summer-fall 2017. In the sex column, F = female and M = male.

Tag No.	Sex	No. filtered locations	No. days tracked	Total distance (km)	Summary period (d)	No. dives	Percent track summarized	Median dives per day	Min. dives per day	Max. dives per day
833	M	84	16.4	642	14.2	1,482	59.1	103	19	188
838	M	33	3.9	273	1.9	195	69.2	36	20	139
848	M	33	4.2	216	2.9	369	88.7	104	19	142
4173	F	44	8.9	548	8.9	997	56.7	118	56	146
4175	F	126	51.6	1,535	51.4	2,985	40.3	67	1	160

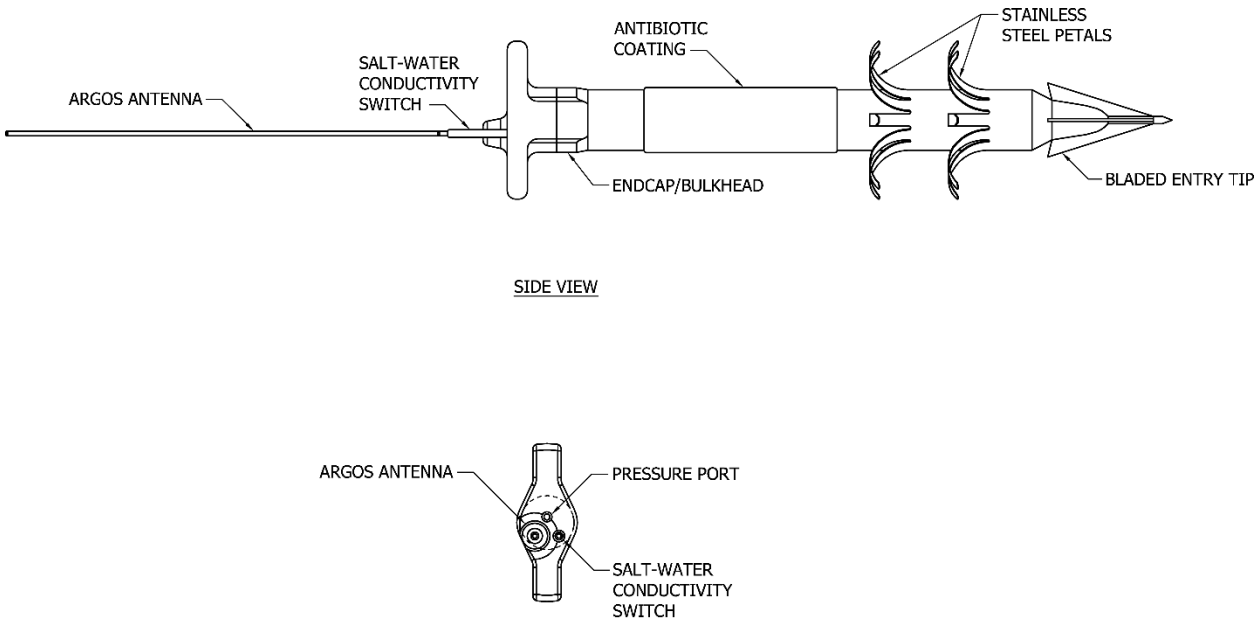

1047

1048

1049 **Figure 1**. Schematic diagram of a fully assembled Telonics RDW-665 tag. Side view (top
1050 drawing) shows the distal endcap with the Argos antenna and saltwater conductivity switch
1051 (SWS), the main body partially coated with antibiotic, and the penetrating tip and anchoring
1052 system with two rows of stainless-steel strips ("petals") in deployed position. Top view (bottom
1053 drawing) shows the placing of the SWS and the pressure transducer. Both views show the two
1054 stop tabs extending laterally from the endcap to prevent the tag from embedding too deeply into
1055 the whale.

1056

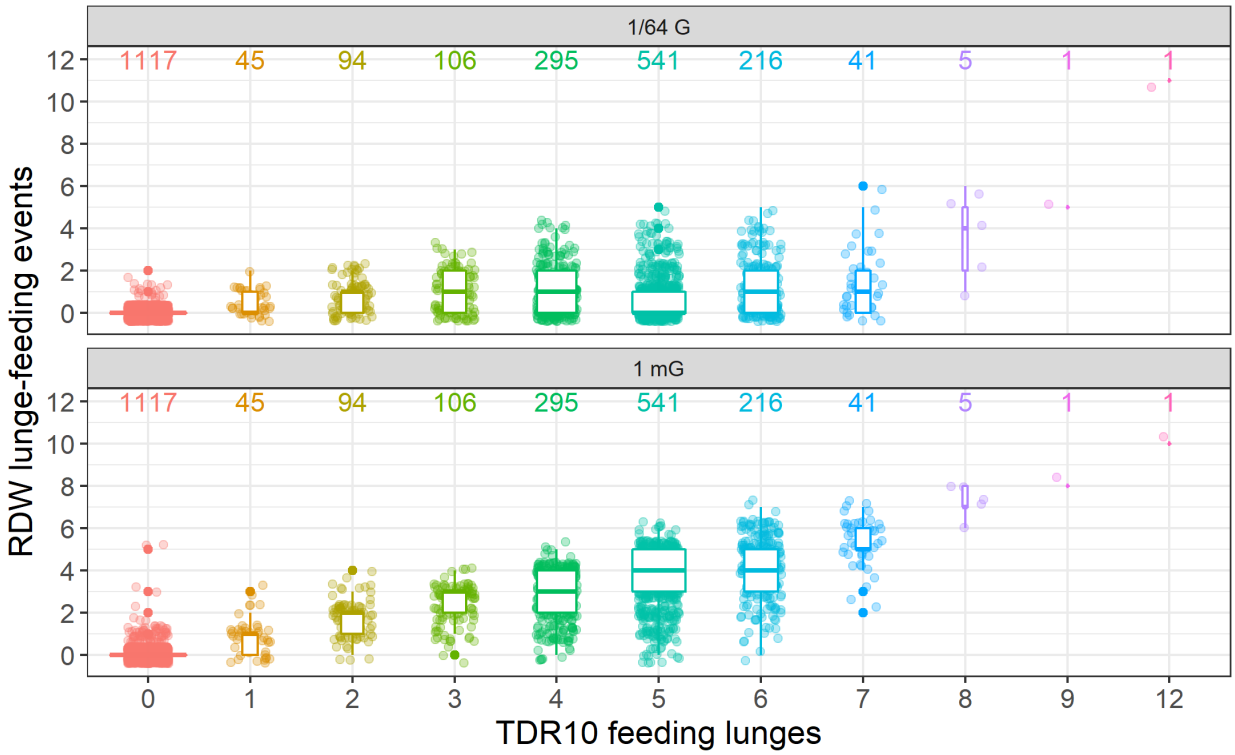

Figure 2. Boxplots of the results of the proxy validation of the RDW tag's event detection algorithm showing the number of detected lunge-feeding events per dive as a function of the known number of feeding lunges per dive determined from a 17.8-d TDR10 archival record of a blue whale. Top panel shows results for 1/64-G data while the bottom panel shows results for 1-mG data. Width of boxes is proportional to the sample size for that category and the numbers at the top of the plot represent the number of dives in that category. Data points are jittered for better visibility.

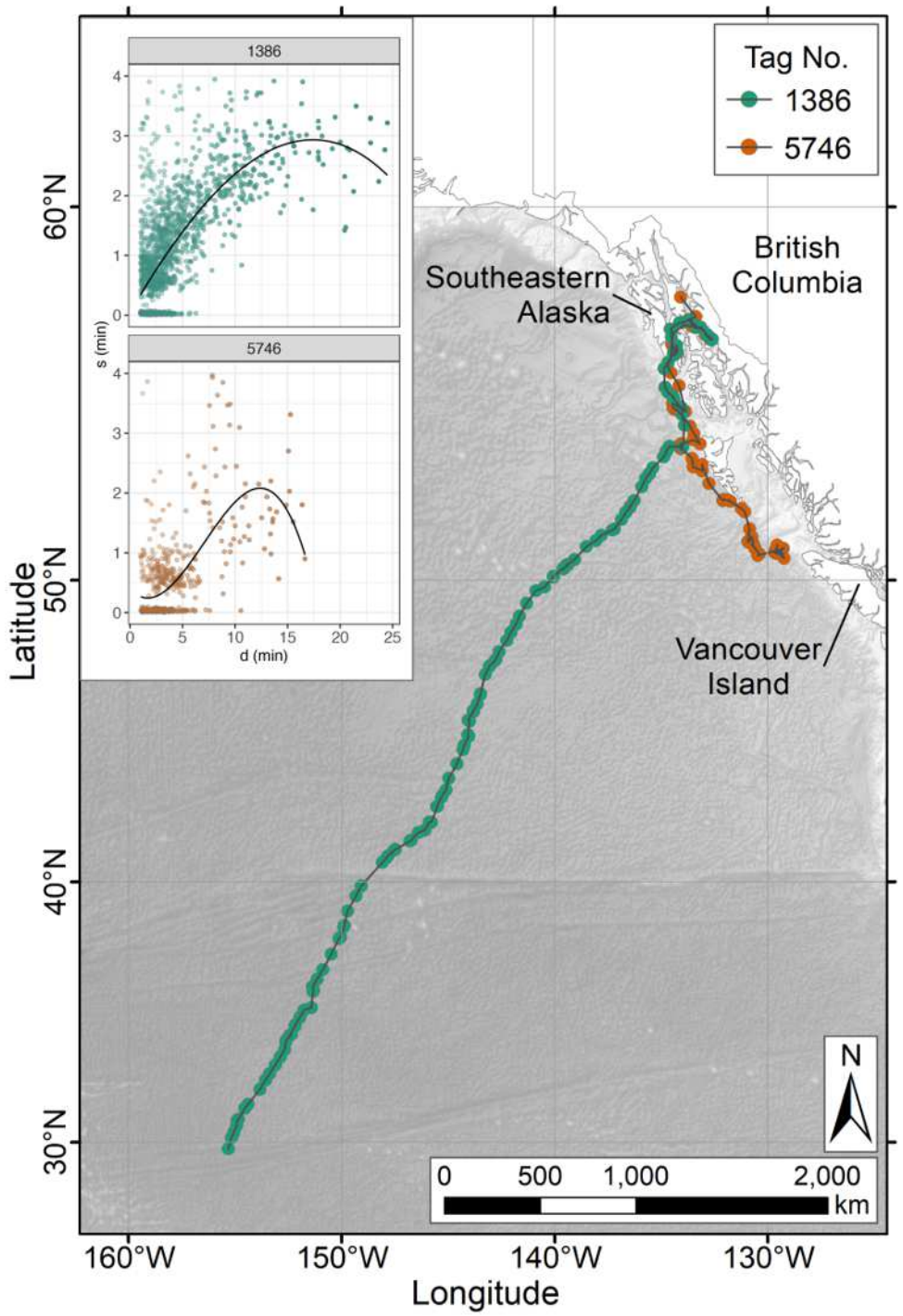

1068

1069

1070 **Figure 3**. The Argos tracks of two humpback whales instrumented with RDW-640 tags in

1071 southeastern Alaska in November 2015. Whale 1386 (a female) was tagged on 17 November

1072 near Petersburg and was tracked for 28 d and 3,980 km while on its breeding migration to
1073 Hawaii. Whale 5746 (of unknown sex) was tagged on 12 November in Seymour Canal and was
1074 tracked for 19 d and 1,657 km as it traveled along the coast toward Vancouver Island. The inset
1075 panels show scatterplots of the relationship between dive duration, *d*, and surface post-dive
1076 interval, *s*, for received dives. The black curve is a cubic spline fit to the data.

1077

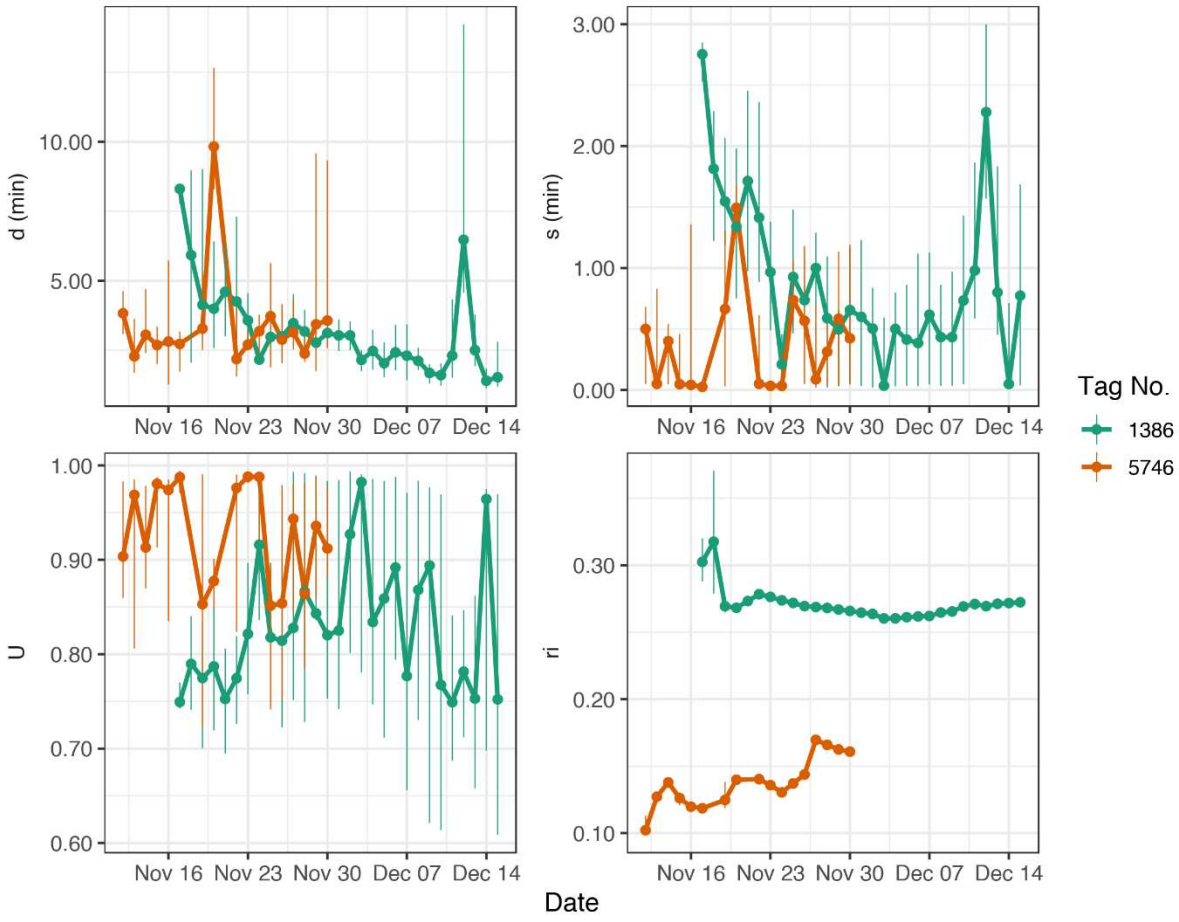

1078

1079

1080 **Figure 4**. The daily median values for dive duration, *d* (top left), surface post-dive interval, *s*
1081 (top right), proportion of time underwater, *U* (bottom left), and ratio of cumulative surface post-
1082 dive interval to cumulative dive duration, r_i (bottom right), for two RDW-640 tags deployed on
1083 humpback whales in southeastern Alaska in November 2015. Vertical error bars around each
1084 daily median value correspond to the inter-quartile range. The tracks of these animals are shown
1085 in Figure 3.

1086

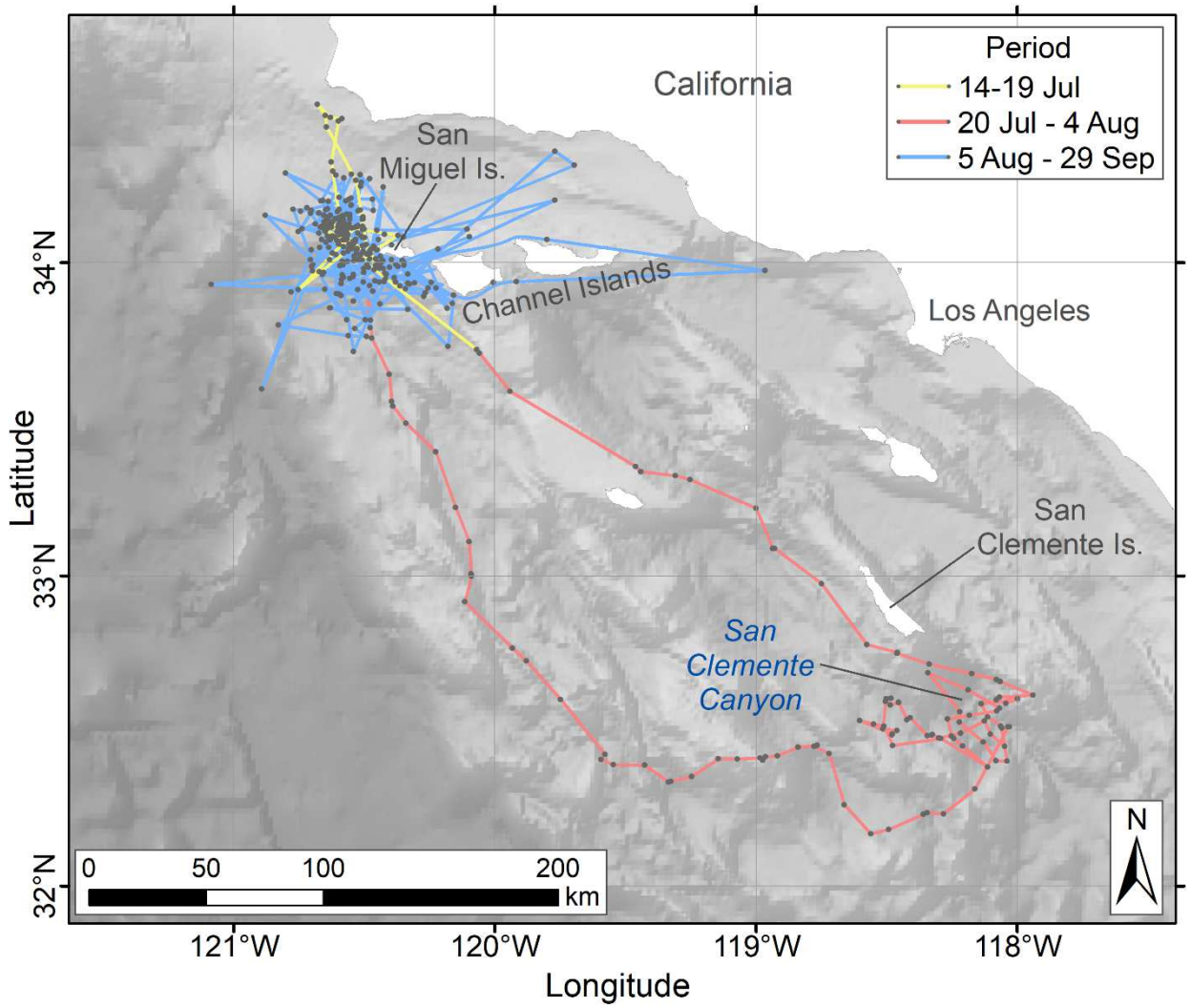

Figure 5. The 76-d Argos track of RDW-665-tagged blue whale 5790 (a male), off southern California during summer-fall 2016. The colored portions of the track correspond to the three periods represented by colored segments along the *x*-axis in Figure 6 (14-19 July, 20 July - 4 August, and 5 August - 29 September).

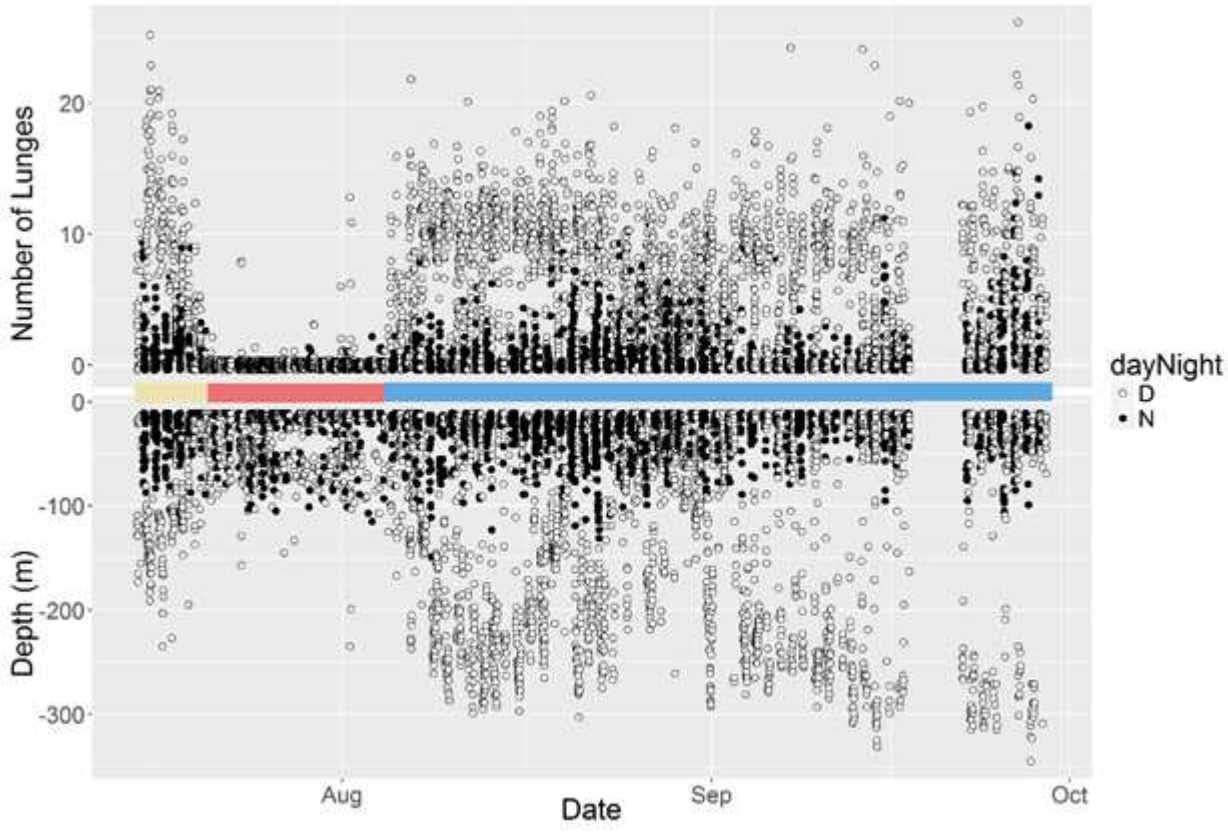

Figure 6. The number of lunges per dive (top panel) and maximum depth of dives (bottom panel) recorded over the 76-d tracking period for RDW-665-tagged blue whale 5790 (a male) in southern California waters during summer-fall 2016. Daytime dives are shown as white circles and nighttime dives as black circles. The data gap in late September was likely due to an issue with the tag's SWS. The three periods represented by colored segments along the *x*-axis (14-19 July, 20 July - 4 August, and 5 August - 29 September) correspond to the portions of track of the same color in Figure 5.

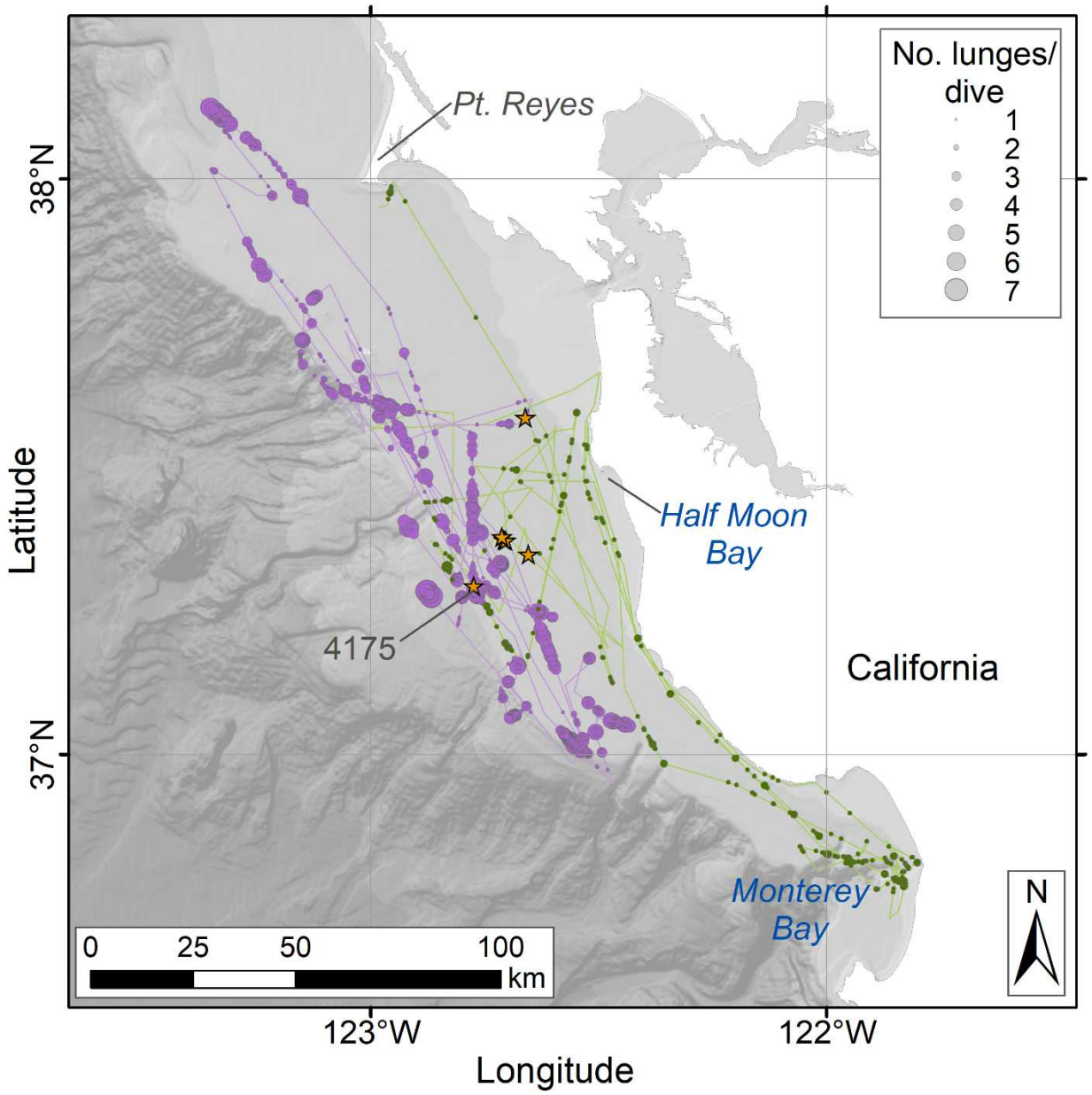

Figure 7. Spatial and individual variability in lunge-feeding events for five RDW-665-tagged humpback whales tracked off central California during summer-fall 2017. Circles identify the interpolated location of feeding dives along the Argos track, with circle size scaled to the number

of lunge-feeding events. For correspondence with how they are discussed in the text, data for tag Nos. 833, 838, 848, and 4173 are shown in green, while data for tag No. 4175 are shown in in purple. Orange stars identify the location of tag deployment.

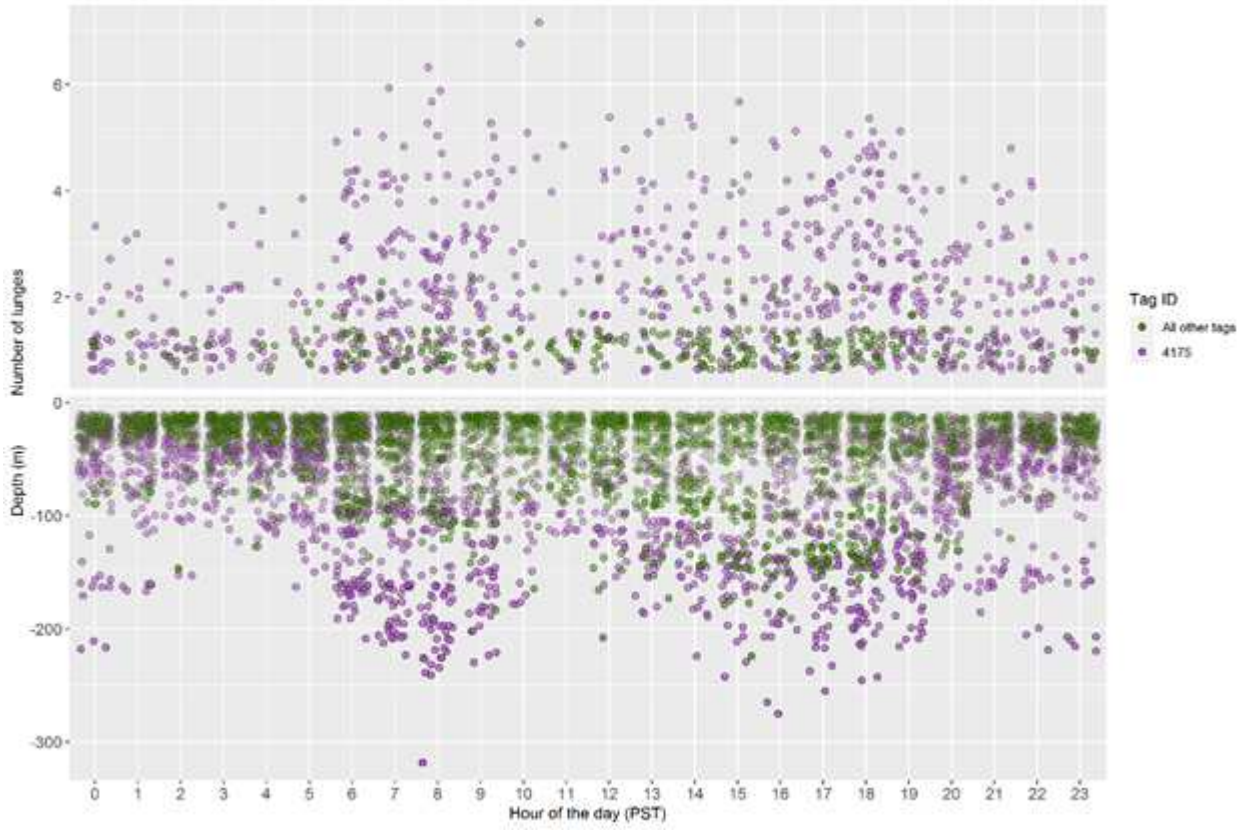

Figure 8. Number of lunges per dive (top panel) and maximum dive depth (bottom panel) by hour of day for five RDW-665-tagged humpback whales tracked off central California during summer-fall 2017, illustrating individual differences in diel variability. For correspondence with how they are discussed in the text, data for tag Nos. 833, 838, 848, and 4173 are shown in green ("all other tags"), while data for tag No. 4175 are shown in purple. Jittering and transparency have been added to reduce overplotting. Fewer dives appear in the top panel because dives that had no lunges are not represented. The tracks of these animals are shown in Figure 7.

Additional file: Additional table and figures

A satellite-linked tag for the long-term monitoring of diving behavior in large whales

Daniel M. Palacios, Ladd M. Irvine, Barbara A. Lagerquist, James A. Fahlbusch, John Calambokidis, Stanley M. Tomkiewicz, and Bruce R. Mate

Preamble

In "*A satellite-linked tag for the long-term monitoring of diving behavior in large whales*," Palacios et al. (2021) present the development of the Telonics RDW tag, a new Argos-based satellite telemetry device that incorporates sensors for monitoring the movements and dive behavior of large whales in near-real-time over several months without requiring recovery. The RDW tag dive summary algorithm was designed to summarize rorqual dive behavior from multiple data streams. It also implements an adaptive event detection algorithm to detect lunge-feeding events from accelerometer data based on thresholds using the running mean and standard deviation of the jerk value. To assess the performance of the RDW tag, we implemented a proxy validation of the tag's dive summary and event detection algorithms using continuously recorded data from a Wildlife Computers TDR10-F medium-duration archival tag deployed on a blue whale (*Balaenoptera musculus*) for 17.8 d while foraging off southern California in summer 2017. We compared dive summaries, including number of lunge-feeding events per dive, generated from the TDR10 archival data to corresponding selected dive summaries produced by the RDW tag dive summary algorithm from the same record. The primary results of this validation are presented in the main text of Palacios et al. Here, we present one table and six additional figures that provide supplementary information relating to the performance of the RDW dive summary and event detection algorithms in the proxy validation, including the variability over time associated with the adaptive event detection thresholds.

Table A1. Summary of RDW event detection algorithm criteria for the five humpback whales presented in case study 3 in the main text. Jerk metrics are in units of 1/64 G s^{-1}. N is the number of utility messages.

Tag ID	N	Elapsed Time (d)	Min. Mean Jerk	Max. Mean Jerk	Min. sd Jerk	Max. sd Jerk	Last Mean Jerk	Last sd Jerk
833	28	12.6	0	15	10	30	11	13
838	3	0.6	15	16	17	18	16	18
848	15	2.1	1	30	2	16	13	15
4173	10	8.1	3	19	9	27	10	11
4175	45	47.5	0	16	7	29	12	13

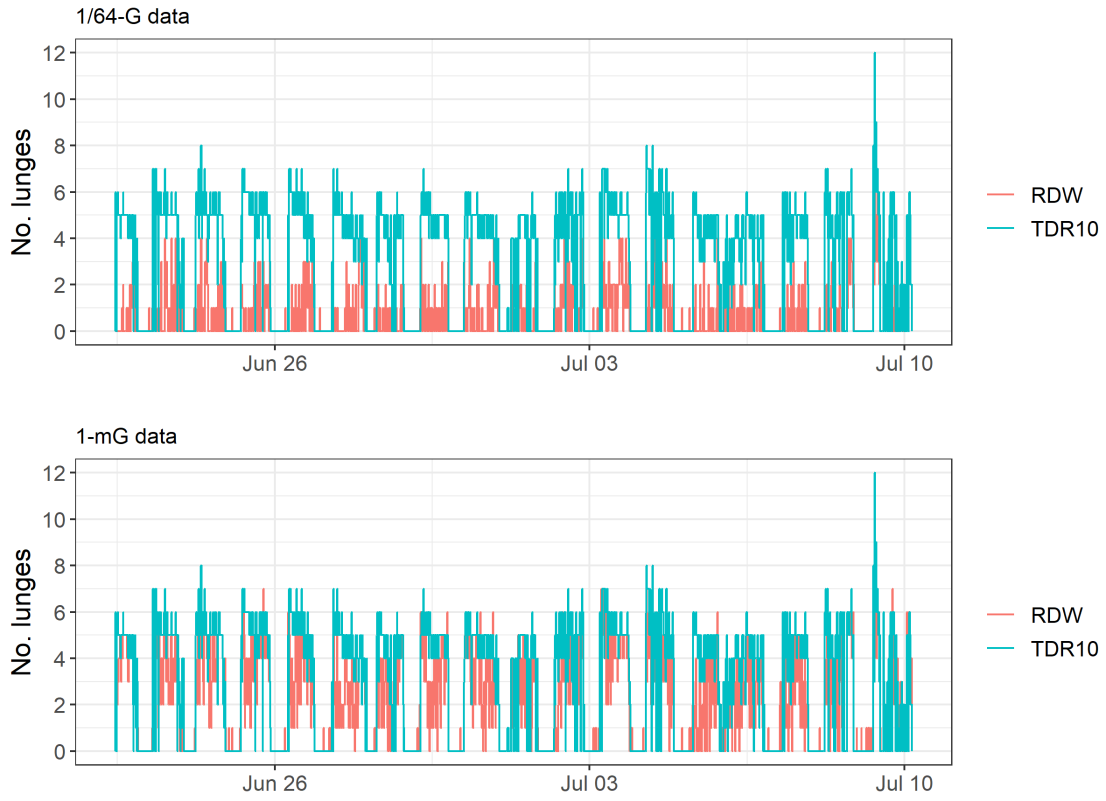

Figure A1. Stairstep plot showing the time series of the number of true feeding lunges per dive measured by a TDR10 archival tag (blue line) and detected by the RDW event detection algorithm (red line). Top panel shows results for 1/64-G precision data while the bottom panel shows results for 1-mG precision data.

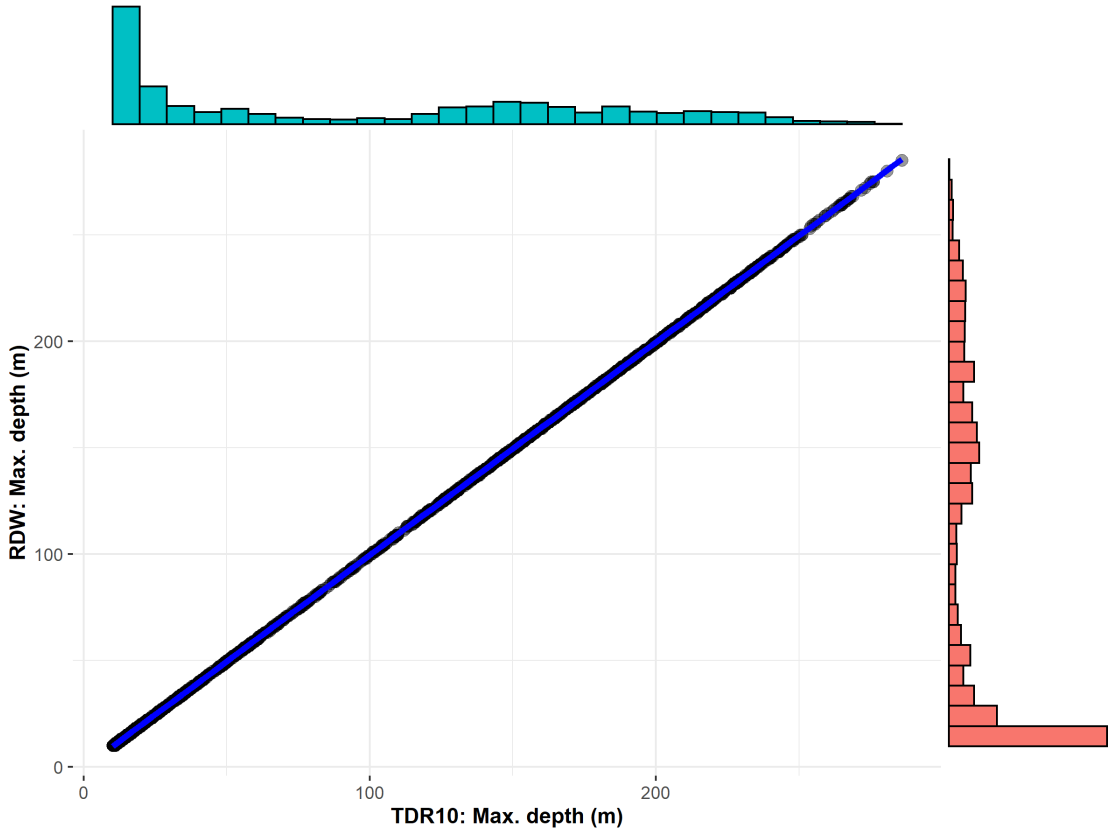

Figure A2. Scatterplot and marginal univariate frequency histograms for the linear regression of maximum dive depth estimated from TDR10 archival tag data to maximum dive depth reported by the RDW dive summary algorithm.

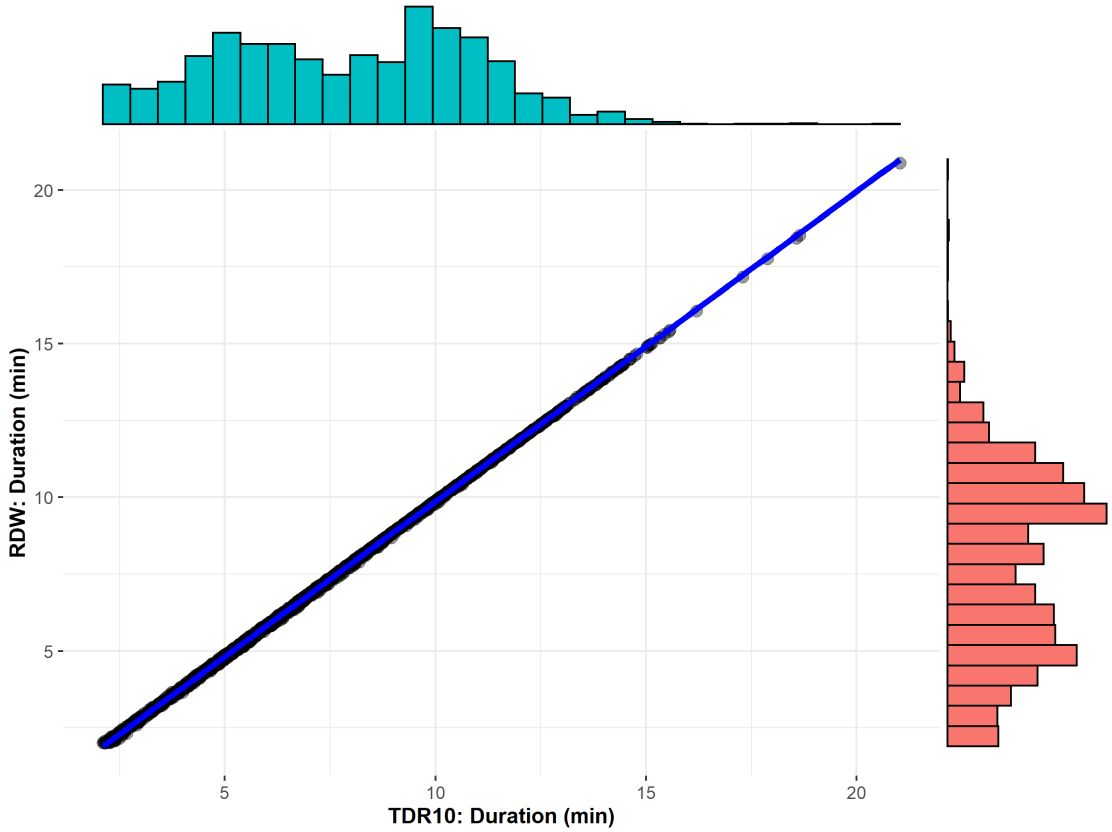

Figure A3. Scatterplot and marginal univariate frequency histograms for the linear regression of dive duration estimated from TDR10 archival tag data to dive duration reported by the RDW dive summary algorithm.

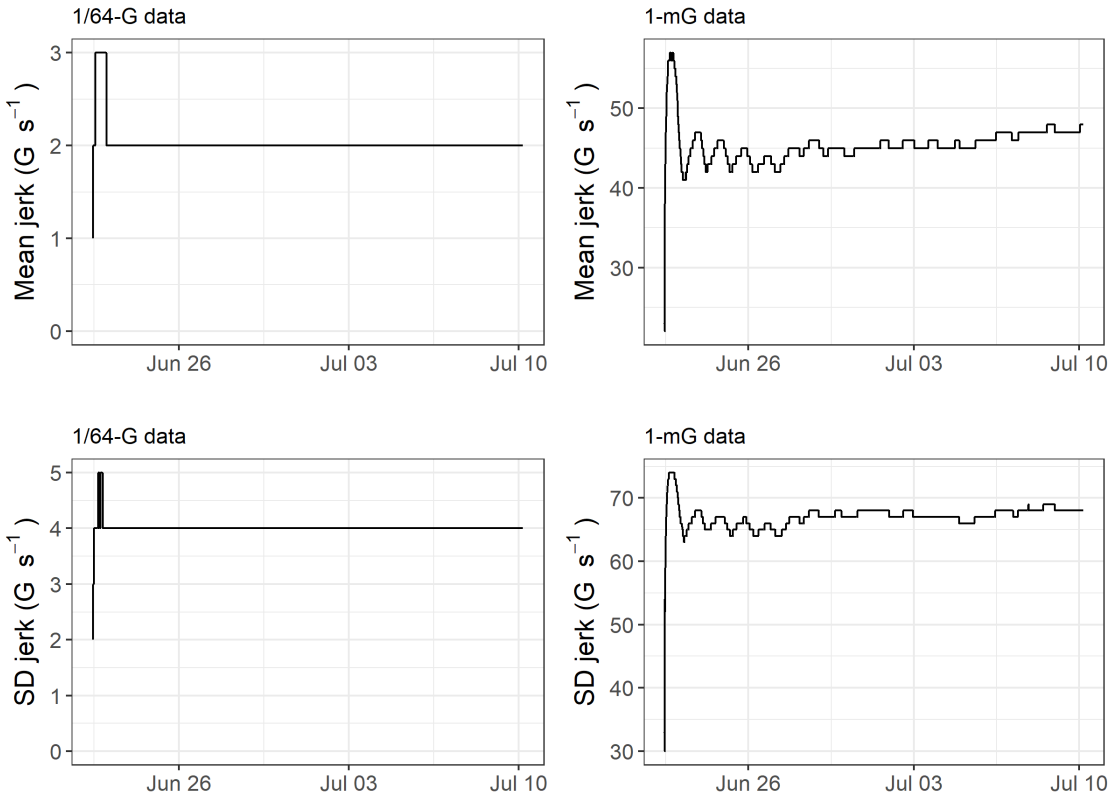

Figure A4. Time series plot of the running mean (top) and standard deviation (bottom) of jerk, used as threshold criteria for lunge-feeding event detection from a TDR10 tag. Left panels display data using 1/64-G precision. Right panels display data using 1-mG precision. Jerk values stabilized after ~ 13 h for 1/64-G data and ~ 19 h for 1-mG data.

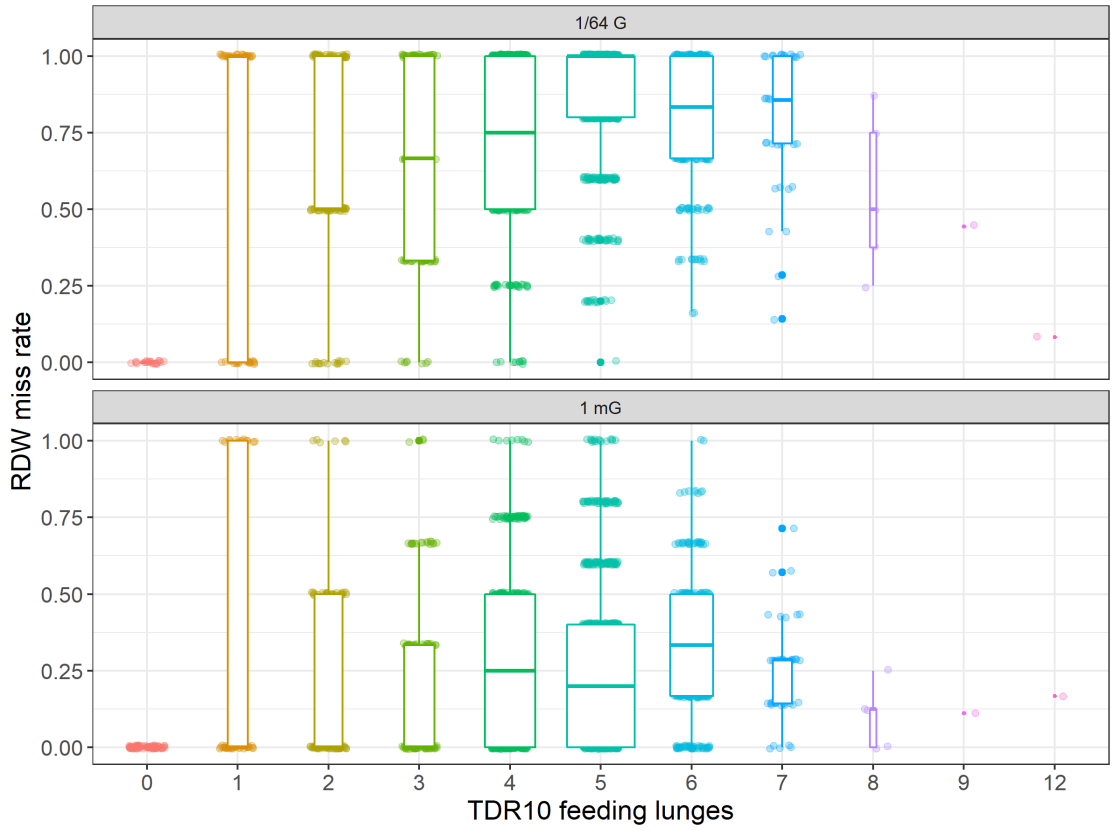

Figure A5. The miss rate (number of false negative lunge events divided by the true number of lunges) of the RDW tag event detection algorithm presented by the number of true lunges per dive measured by the TDR10 tag. Top panel displays results using 1/64-G precision data and the bottom panel displays results using 1-mG precision data.

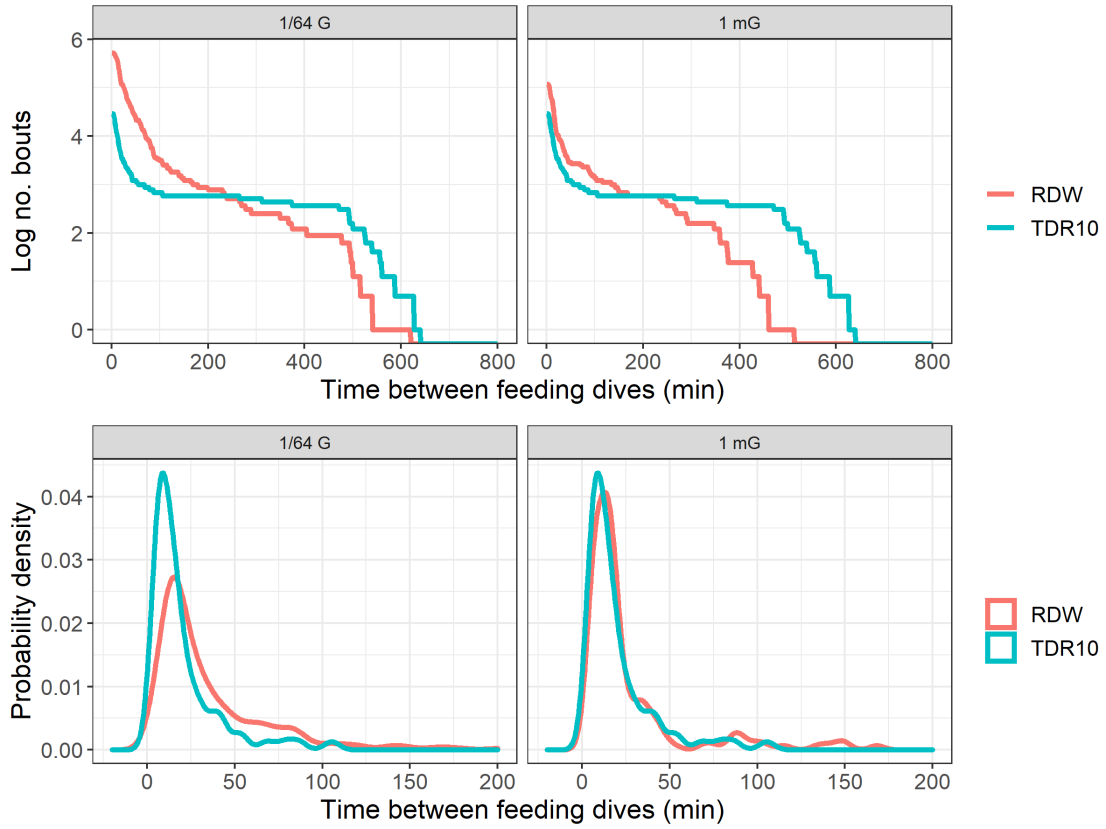

Figure A6. Log-survivorship curves showing the number of feeding bouts as a function of time between feeding dives (top) and probability density of times between feeding dives (bottom) measured by a TDR10 archival tag (blue line) and detected by the RDW event detection algorithm (red line). The two plots are used in establishing a criterion to distinguish between bouts of feeding dives, which for this example was 60 min between feeding dives. Left panels show results for 1/64-G precision data while the right panels show results for 1-mG precision data.